# I A V C E I
## CANBERRA 1993

# EXCURSION GUIDE

## RABAUL CALDERA - PAPUA NEW GUINEA

Compiled by Chris McKee,
with contributions from Ian Nairn, Peter Wood, Ben Talai and George Walker

Record 1993/69
Australian Geological Survey Organisation

## DEPARTMENT OF PRIMARY INDUSTRIES AND ENERGY

Minister for Resources: Hon. Michael Lee
Secretary: Greg Taylor

## AUSTRALIAN GEOLOGICAL SURVEY ORGANISATION

Executive Director: Harvey Jacka

© Commonwealth of Australia

**ISSN: 1039-0073**

**ISBN: 0 642 19670 2**

This work is copyright. Apart from any fair dealings for the purposes of study, research, criticism or review, as permitted under the Copyright Act, no part may be reproduced by any process without written permission. Copyright is the responsibility of the Executive Director, Australian Geological Survey Organisation. Inquiries should be directed to the **Principal Information Officer, Australian Geological Survey Organisation, GPO Box 378, Canberra City, ACT, 2601.**

IAVCEI GENERAL ASSEMBLY, CANBERRA 1993

# Field Trip C1: Rabaul Caldera

Compiled by

Chris McKee, Rabaul Volcano Observatory

with contributions from

Ian Nairn & Peter Wood, Institute of Geological & Nuclear Sciences
Ben Talai, Rabaul Volcano Observatory
George Walker, University of Hawaii

CONTENTS


| | Page |
|---|---|
| Introduction | 1 |
| Regional Geology | 1 |
| Topography | 2 |
| Geology | 6 |
| Lavas | 6 |
| Pyroclastics | 7 |
| (i) Ignimbrites | 8 |
| (ii) Plinian deposits | 9 |
| (iii) Welded and unwelded scorias | 9 |
| (iv) Fine grained vitric ashes | 11 |
| Sediments | 11 |
| Petrology | 11 |
| Raluan Pyroclastics | 18 |
| Structure | 18 |
| Eruptive History | 20 |
| Pre-historical Activity | 20 |
| Historical Activity | 20 |
| Volcano Surveillance | 22 |
| Seismology | 22 |
| Ground Deformation | 24 |
| (i) Uplift | 25 |
| (ii) Tilt | 26 |
| (iii) Horizontal deformation | 26 |
| Gravity | 27 |
| Acknowledgements | 28 |
| References | 29 |
| Excursion Route - Stop Descriptions | 31 |

## INTRODUCTION

Rabaul township and associated villages (population about 70,000) are situated precariously within and around an active caldera complex. The most recent damaging eruptions at Rabaul took place in 1937 when centres on opposite sides of the caldera were simultaneously active. About 500 lives were lost in the Vulcan eruption of that year. Rabaul Volcano Observatory (RVO) was established soon afterwards to monitor activity and to provide warnings of future eruptions.

Geophysical monitoring and geological studies at Rabaul have made significant progress in the past few decades, although much remains to be learned about the dynamics and the geology of this complex volcano. Surveillance since 1971 has revealed on-going uplift of part of the caldera floor and variable rates of seismicity around the edges of an elliptical cylindrical structure believed to define the caldera bounding fault(s). Early studies of the geology and volcanology of Rabaul (Fisher, 1939; Heming, 1974) concentrated on relatively recent events which are dominated by a caldera-modifying eruption 1400 yrs BP. Later work (Walker et al., 1981; Nairn et al., 1989) demonstrated that Rabaul Volcano is essentially an ignimbrite shield. Its eruptive history spans about 0.5 Ma and includes many ignimbrite-producing, caldera-forming eruptions.

On a global scale, the activity at Rabaul is of major significance. In a world-wide study of historical unrest at large calderas, Newhall & Dzurisin (1988) suggested that the unrest at Rabaul was perhaps the most threatening example studied by them. A number of factors raise concern at Rabaul, specifically, caldera-forming eruptions only 6,800 and 1,400 years ago, simultaneous eruptions on opposite sides of the caldera in 1878 and 1937, and the pattern of ground deformation and seismicity within the caldera. This excursion guide provides a summary of current knowledge of Rabaul Volcano and may help to focus future efforts to improve our understanding of its evolution.

## REGIONAL GEOLOGY

Rabaul Volcano, at the northeastern tip of the Gazelle Peninsula in eastern New Britain (Fig. 1), lies in the zone of island arcs and oceanic crust which makes up the northeastern part of Papua New Guinea (Johnson, 1979). Tectonically, this is the most active part of the country. A zone of intense seismicity and volcanism marks the northern margin of the Solomon Sea Plate where it is being subducted beneath New Britain and Bougainville. There is a sharp (80°) flexure in the Benioff zone between New Britain and Bougainville. In the plate(s) overlying this spur on the Benioff zone,

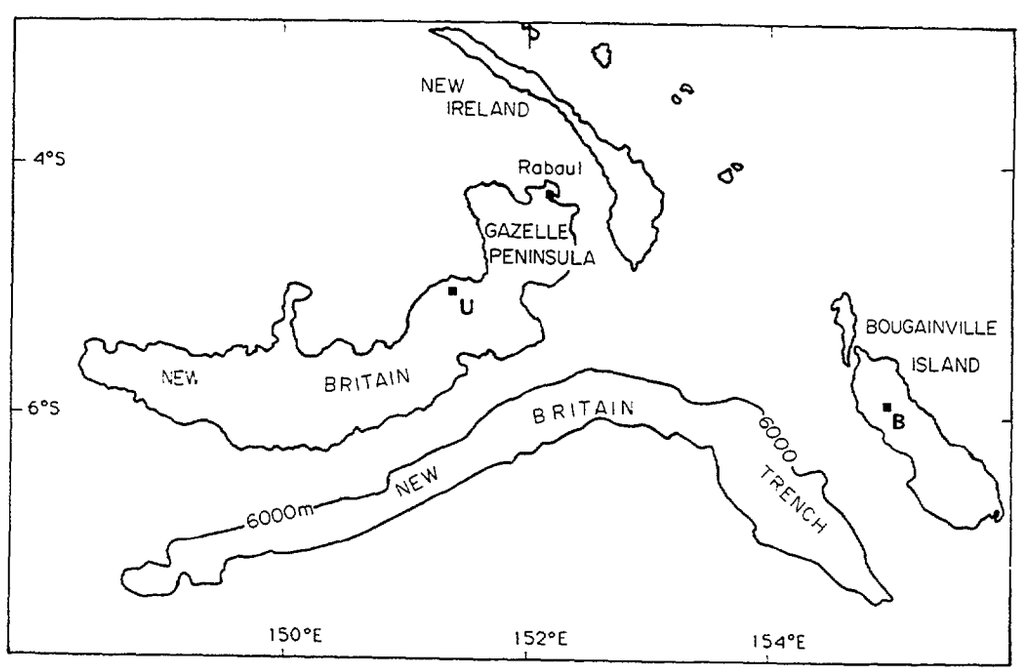


*Fig. 1. Islands region of Papua New Guinea showing Rabaul at the northeastern tip of the Gazelle Peninsula, New Britain. The locations of the volcanoes Ulawun (U) and Balbi (B) are also shown.*

there is a region of intense fracturing (the Gazelle Peninsula) and a paucity of active volcanoes (Rabaul is the only active volcano between Ulawun in east-central New Britain and Balbi in northern Bougainville).

The regional geology of the Gazelle Peninsula has been described by Macnab (1970), Davies (1973) and Lindley (1988). Basement in the Gazelle Peninsula (and elsewhere in New Britain) consists of the Late Eocene basic to intermediate volcanics and derived sediments of the Baining Volcanics. This formation is unconformably overlain by the Late Oligocene Merai Volcanics of similar lithology. Dioritic intrusions in the Late Oligocene preceded the development in the Early Miocene of an extensive carbonate platform, whose main element is the Yalam Limestone. The Baining Mountains Horst and Graben Zone (Lindley, 1988), localized a number of emergent volcanic centres in the east-central part of the Gazelle Peninsula in the Middle Miocene - Pliocene (Fig. 2). The oldest of these volcanic centres is the Nengmutka Caldera to the south. The products of these centres, the Nengmutka Volcanics, comprise andesitic lavas and pyroclastic flow deposits, rhyolitic lavas and derived sediments. Partly coeval with this formation is the Arabam Diorite. The Sinewit Formation, also of Miocene - Pliocene age, is laterally equivalent with the Nengmutka Volcanics and is dominated by volcaniclastic sandstone and siltstone. The suggestion of northward-migrating volcanism evident in the Late Tertiary became stronger in the Quaternary.

A north-trending belt of volcanic centres developed in the Rabaul region in the Quaternary, apparently as an outgrowth on the Late Tertiary northeastern coast of the Gazelle Peninsula. The Rabaul region is defined as the area lying north of the Warangoi and Nengmutka Rivers and east of the Vudal River (Fig. 3). The southern-most volcanic centre in the Rabaul region formed the subcircular 11 km wide "Varzin Depression" (Fig. 3; Nairn et al., 1989). This feature is delineated on its northeastern side by a 6 km-long northwest-trending eroded scarp, part of the "Toma Fault" (Nairn et al., 1989). The remaining outline of the Varzin Depression is completed by arcuate lineations formed by deep stream channels. Other concentric arcuate lineations are present within the depression (Fig. 4). Mt. Varzin is a small eroded basaltic cone near the eastern margin of the depression. Another similar but smaller cone, Wairiki, lies 4 km to the southeast. Pyroclastics from the Varzin Depression centre have not yet been positively identified. However the Toma Fault exposes the oldest pyroclastics in the Rabaul region, which are informally known as the "Toma Volcanics" (Nairn et al., 1989), and these deposits are regarded as being products of an early collapse structure at the site of the Varzin Depression. This structure has largely been infilled by products from Mt. Varzin and by ignimbrites from younger centres to the north (including Rabaul Volcano).

Immediately north of the Varzin Depression is the 3 x 4 km "Vunakanau Basin" (Fig. 3; Nairn et al., 1989). This shallow depression, rimmed by Toma Volcanics on its southern side and a ridge of rocks from Rabaul Volcano on its northern side, has also been infilled by young ignimbrites. The basin topography and drainage radial to it are suggestive of another pre-Rabaul Volcano eruptive centre. Some of the oldest units exposed within the Rabaul Caldera, adjacent and northeast of the Vunakanau basin, are thickest or present only in the southern part of the caldera, leading to the possibility that they may have originated from a Vunakanau source.

The Late Cainozoic pattern of northward-younging volcanic centres in the northern part of the Gazelle Peninsula is upset by the development of Tovanumbatir Volcano prior to the commencement of activity at its adjacent southern neighbour Rabaul Volcano. Also upsetting the migration pattern is the apparently simultaneous development of the Rabaul centre and the newly discovered submarine "Tavui Caldera" (Taylor et al., 1991) immediately north of Rabaul (Fig. 3). The Tavui Caldera is approximately circular having a diameter of about 9 km. The featureless central part of the floor of the caldera lies about 1100 m below sea level. Several intra-caldera centres appear to have formed in the northeastern sector of the caldera. Tavui Caldera's northern rim nearly reaches the surface of the sea, while its southwestern wall is partly subaerial, expressed as the "Tavui Fault" (Nairn et al., 1989). The Tavui Fault cuts through early Rabaul-sourced pyroclastics, but no deposits have yet been identified as originating from Tavui Caldera. About 10 km west of Tavui Caldera is Watom Island (Figs. 3,4). Of volcanic origin, Watom has a broad crater about 2 km wide and is deeply dissected. Watom has a collar of raised coral reef and its age may be similar to that of Tovanumbatir.

## TOPOGRAPHY

The main topographic features at Rabaul are: a largely sea-filled caldera which measures 14 x 9 km, the high cones Kombiu (664 m a.s.l.), Tovanumbatir (532 m a.s.l.), and Turangunan (482 m a.s.l.), the nested craters Palangiagia and Rabalanakaia, the intra caldera centres Tavurvur (232 m a.s.l.) and Vulcan/Vulcan Island (225 m a.s.l.), and a peninsula extending from the northeastern part of the caldera southward to near its centre (Fig. 5).

In the northeast and east the topographic wall of the caldera is a single near-vertical scarp. In the west two scarps are present, partially draped by younger pyroclastic deposits. Breaching of a 5 km long section of the caldera's southeastern wall has led to the formation of Blanche Bay.

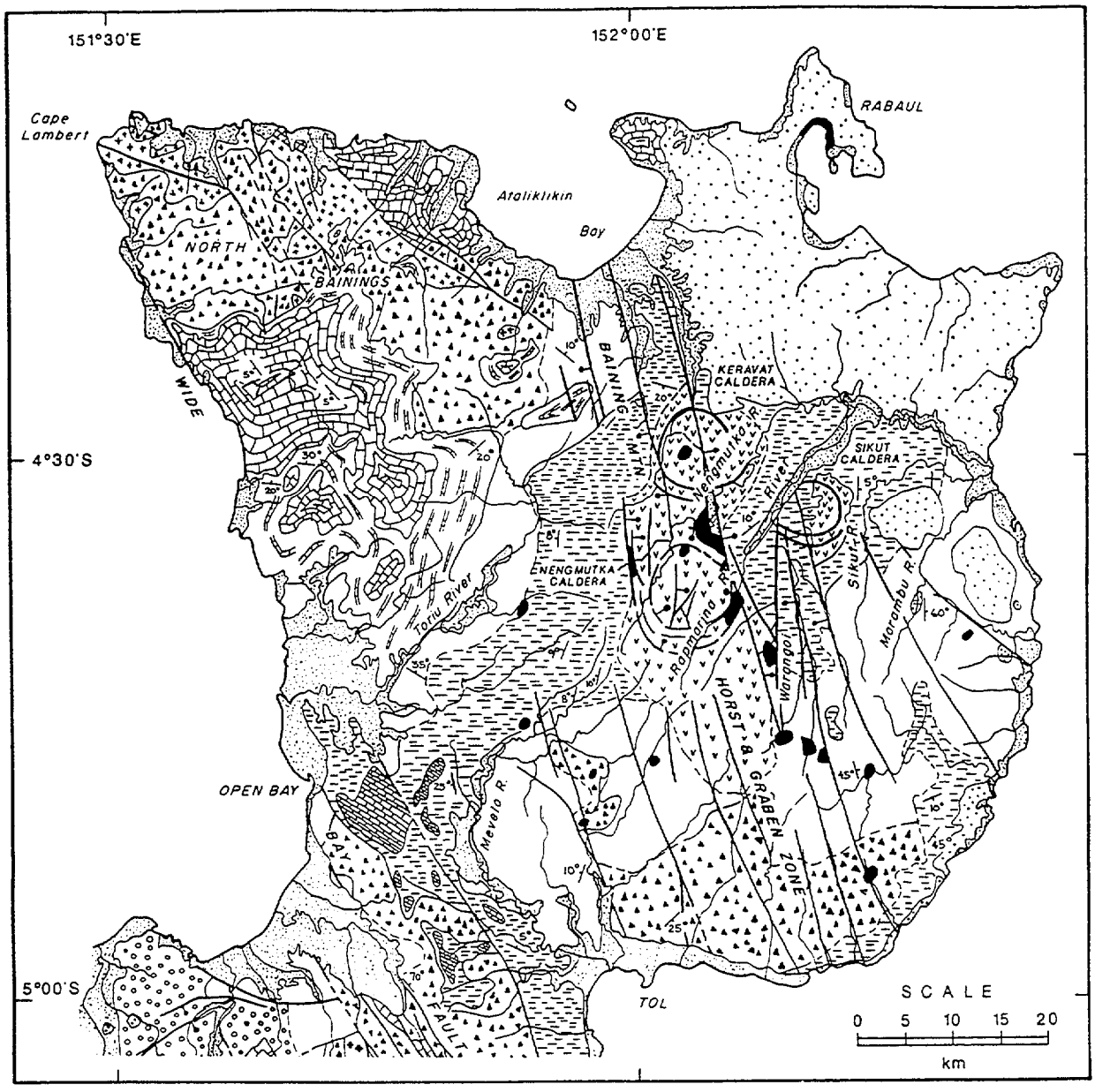


QUATERNARY

*Alluvium and beach sand*

*Undifferentiated*

PLIOCENE

LAKIT LIMESTONE. *White bioclastic limestone, occasionally poorly consolidated*

MIO-PLIOCENE

SINEWIT FORMATION. *Poorly to partly consolidated sandstone, minor limestone and breccia*

NENGMUTKA VOLCANICS. *Andesite, ashflow tuff, flow-banded rhyolite and siltstone*

EARLY TO MIDDLE MIOCENE

YALAM LIMESTONE. *Bioclastic limestone with interbeds of chalky limestone*

BERGBERG FORMATION. *Calcareous sandstone and mudstone; carbonaceous horizons*

PALI RIVER CONGLOMERATE. *Conglomerate, sandstone and minor shale and coal*

MID-MIOCENE

ARABAM DIORITE. *Coarse-grained quartz diorite*

LATE OLIGOCENE

*Diorite, leucogabbro and microdiorite*

ESIS-SAI INTRUSIVE COMPLEX. *Diorite, leucogabbro and microdiorite*

MERAI VOLCANICS. *Lithic tuff, andesite, breccia, basalt; minor limestone*

LATE EOCENE

BAINING VOLCANICS. *Indurated breccia, tuff, andesite and basalt*

*Fig. 2. Tertiary volcanic centres in the east-central part of the Gazelle Peninsula (after Lindley, 1988).*

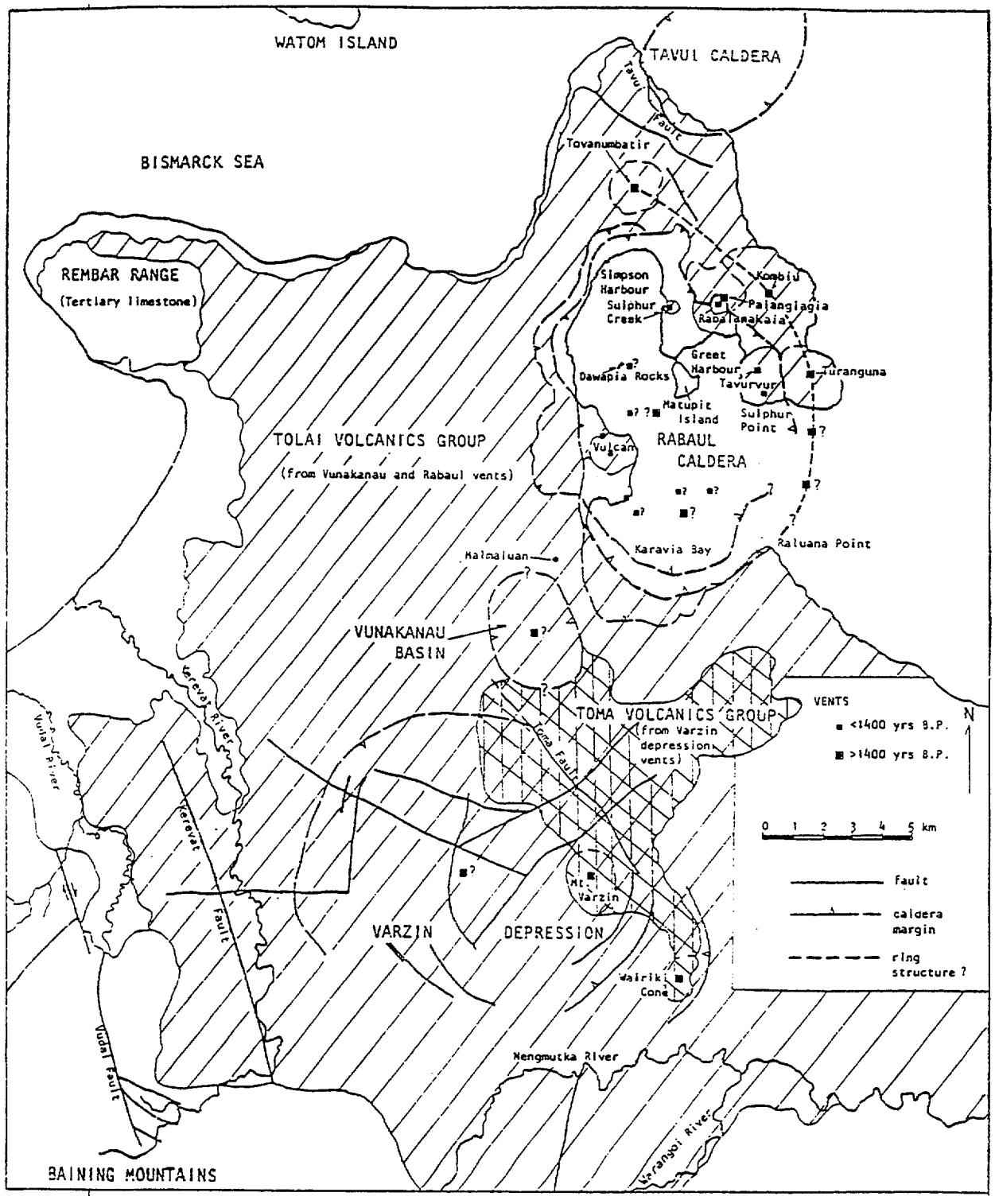


*Fig. 3. Quaternary volcanic centres in the Rabaul region (after Nairn et al., 1989).*

Much of the caldera floor topography (Fig. 6) resulted from activity following the latest caldera-forming eruption (c.1400 yrs BP). A north-south trending trough drains south from Simpson Harbour into a somewhat closed basin in Karavia Bay (the deepest part of the caldera at 295 m below sea level). To some extent, position and shape of the trough are controlled by the post-caldera growth of the Dawapia Rocks, Vulcan Island, Vulcan Cone, and their related deposits, and the uplift and eruptive activity which has occurred in the Matupit Island-Sulphur Creek area. Greet Harbour occupies a crater-like depression, but no ejecta from a source in this area has yet been identified. Alternatively, Greet Harbour might represent a depressed area left after uplift and/or volcanism at the surrounding areas of Matupit Island-Sulphur Creek, Rabalanakaia and Tavurvur. A line of submarine peaks

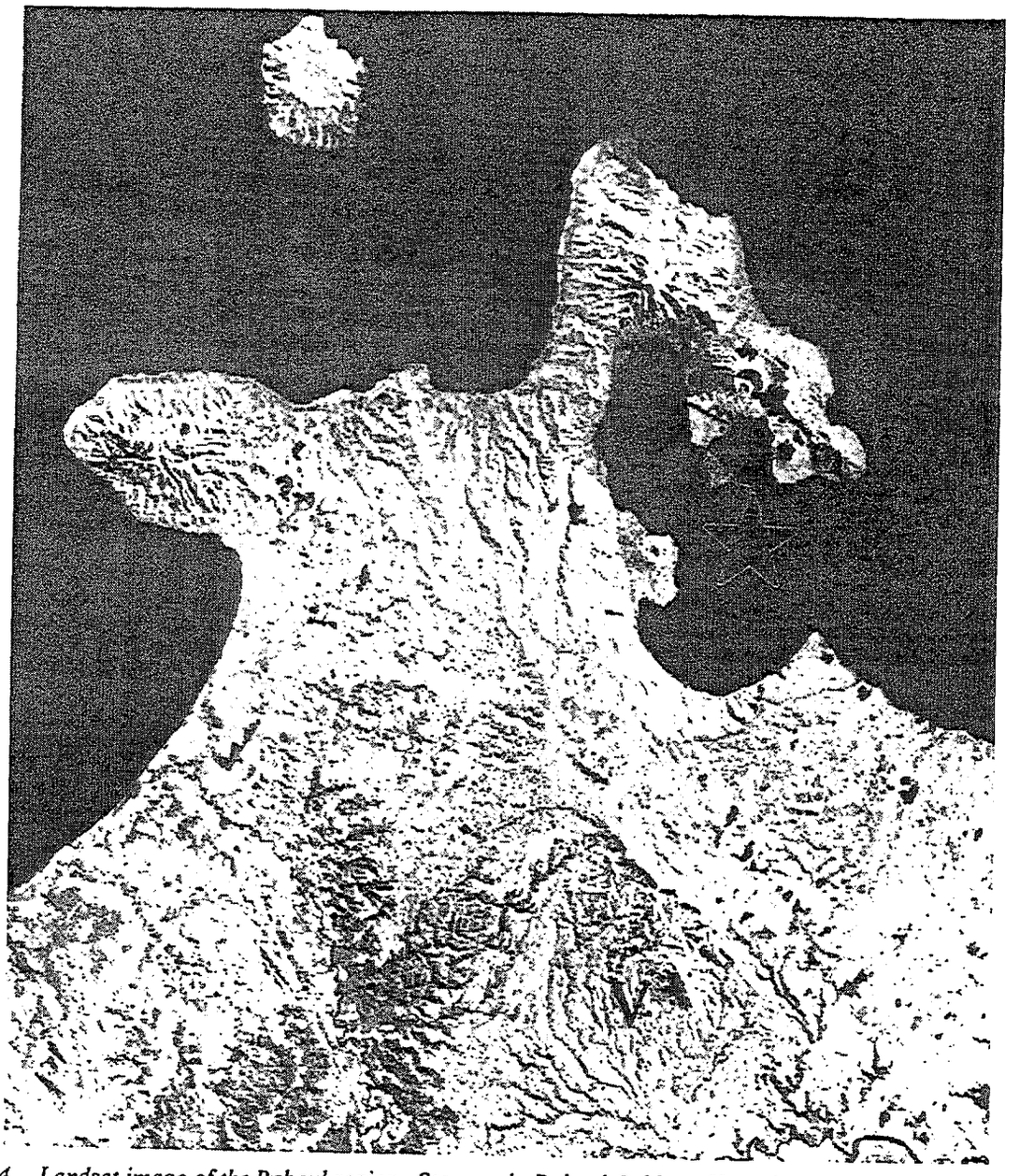

*Fig. 4. Landsat image of the Rabaul region. Star marks Rabaul Caldera, V marks Varzin Depression.*

east of the Vulcan Island vent may indicate a post-caldera volcanic vent lineation. Other small vents lie to the north and south of the Vulcan headland. The submarine peaks immediately south of Turangunan are parts of the submerged southeastern caldera rim and probably pre-date the latest caldera-forming episode. It remains possible, however, that these peaks are parts of discrete volcanoes.

Tovanumbatir is a deeply dissected extinct volcano which pre-dates the Rabaul caldera complex, and has a thick mantle of Rabaul tephra on its lower flanks. On the other hand, Kombiu and Turangunan are much younger volcanoes, having developed as satellite centres on the flanks of the Rabaul complex. They are much less dissected and have relatively thin, patchy deposits of the latest Rabaul tephra units.

The area north and west of the caldera is characterized by strongly dissected topography, typically with sharp main ridges between deep v-shaped valleys which extend close to the present coast. In the main drainage channels to the west of the caldera, some of these v-shaped valleys are infilled by young ignimbrites, which themselves have been partially eroded to form narrow, vertical-walled canyons.

The drainage patterns on the western and southern flanks of the Rabaul complex are tangential to the caldera (Fig. 5) and originate from an area of high ground (about 400 m a.s.l.) immediately southwest of Rabaul. These features are interpreted as evidence for a pre-Rabaul low angle shield volcano (Vunakanau). It is believed that the Rabaul system developed on the northeastern flank of the earlier volcano which has been largely obliterated by Rabaul deposits.

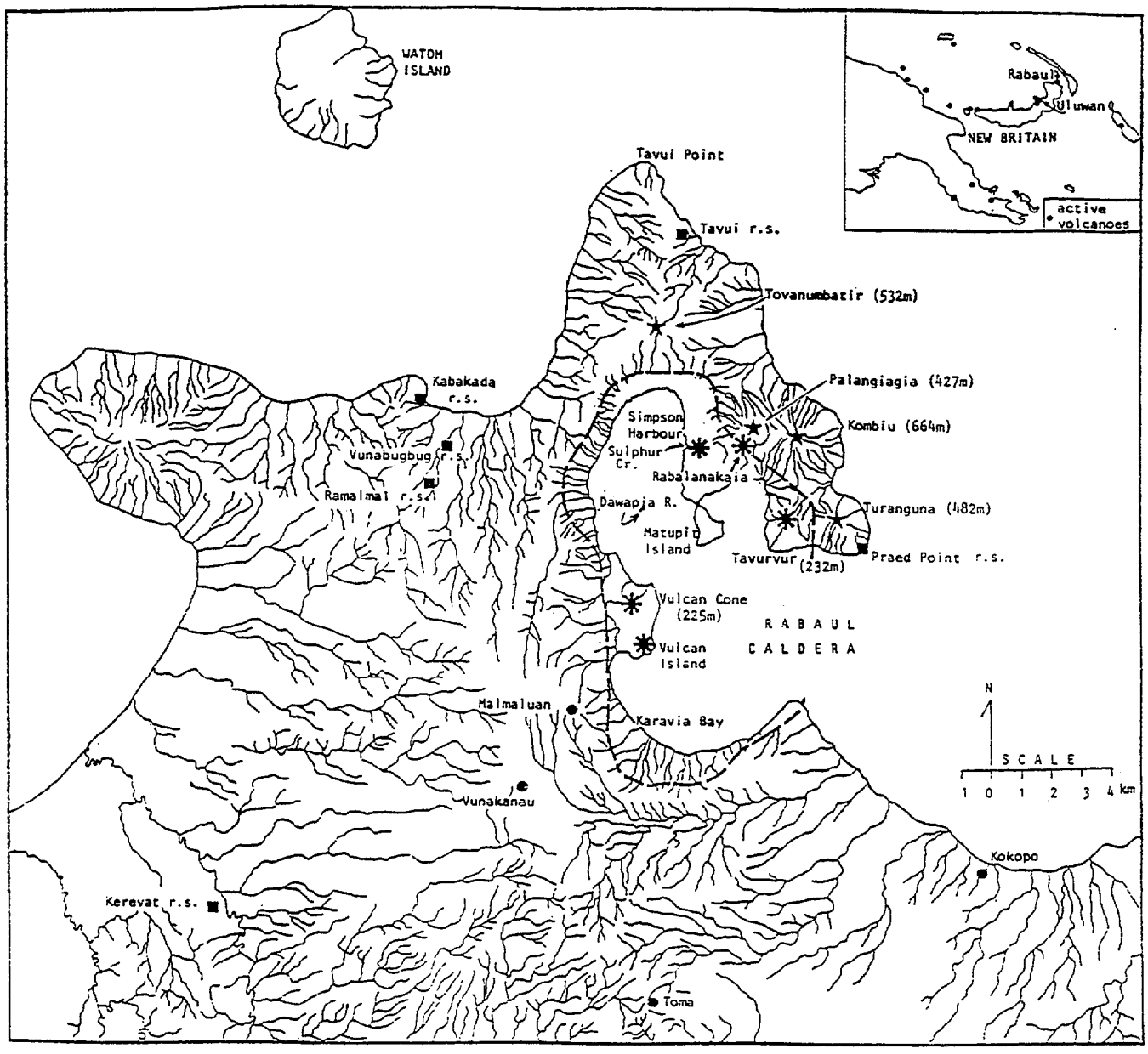


*Fig. 5. Topography of the Rabaul area (after Nairn et al., 1989) showing drainage, locations of stratigraphic reference sections (filled squares), pre-caldera volcanoes (stars), and the main post-caldera volcanic vents (asterisks).*

## GEOLOGY

The geology of Rabaul is largely the product of two main types of volcanism: (a) basaltic and basaltic andesite cone building eruptions, and (b) dacitic, and rarely andesitic or rhyolitic plinian/ignimbrite eruptions. Thus, in general, the geology can be described in terms of lavas and pyroclastics. Sediments constitute a minor component of the geology of Rabaul.

### Lavas

The oldest exposed lava bodies are the basaltic lavas from the pre-caldera Tovanumbatir cone (K-Ar dated at c. 0.5 Ma), and the Seismograph Lavas (source unknown) in the base of the eastern wall of the caldera.

Overlying these units respectively are the dacitic Rabaul Quarry Lavas and East Wall Lavas. These lava bodies are strongly jointed, displaying arcuate and circular joint patterns as well as platy jointing. Exposures in the caldera walls are as much as 80 m high. They are similar chemically and petrographically and are the only known dacitic lava flows at Rabaul. The sources of these lavas are unknown but were probably located within the area of the caldera. A K-Ar date of c. 0.19 Ma has been obtained for the Rabaul Quarry Lavas.

Kombiu, Palangiagia and Turangunan Lavas, together with scoria and ash deposits, make up the satellite cones of the same names. These lavas are basaltic and

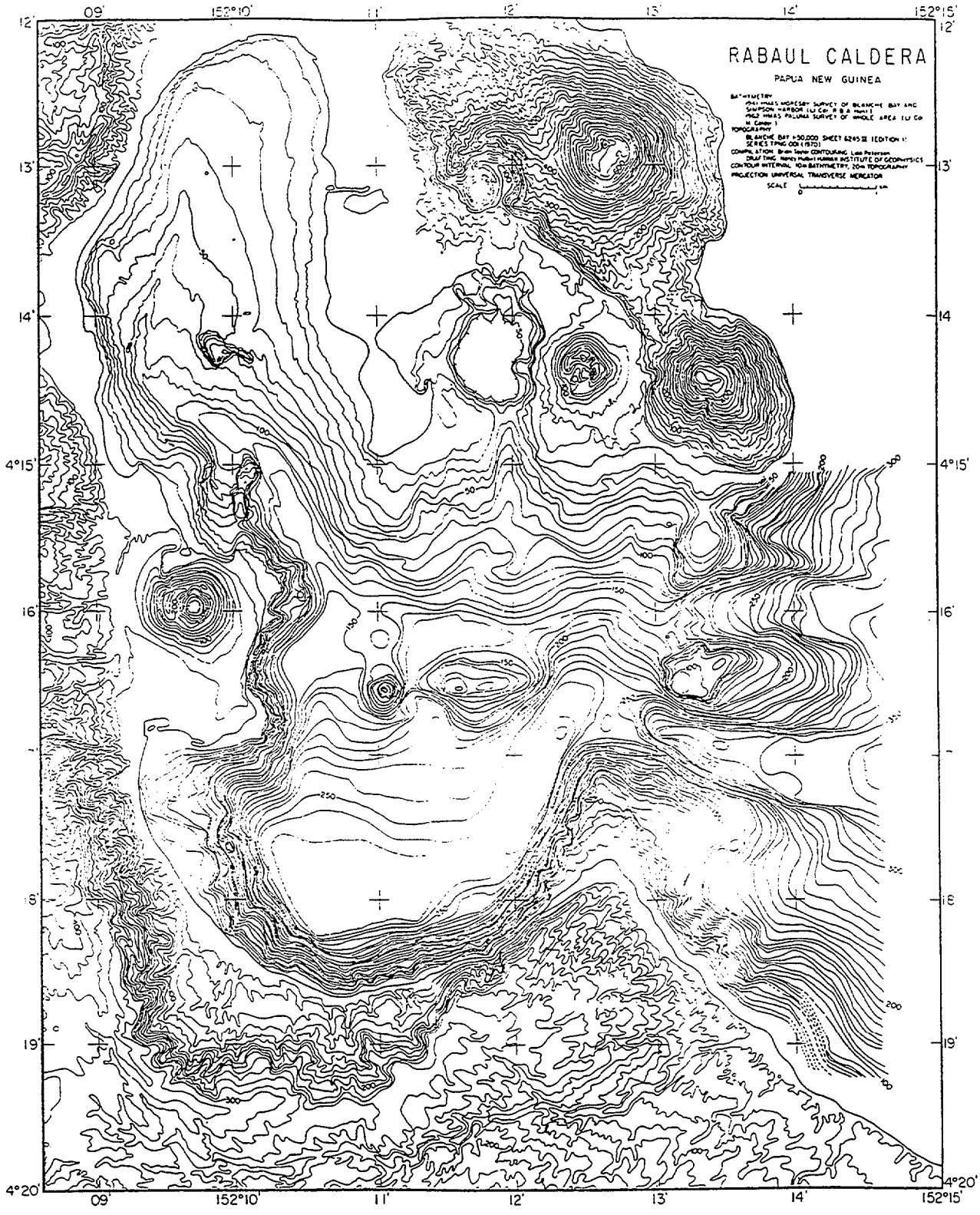


*Fig. 6. Bathymetry of Rabaul Caldera (reproduced with the permission of Hawaii Institute of Geophysics).*

include massive, vesicular, scoriaceous and brecciated lithologies.

The youngest lavas are from the post-caldera centres Rabalanakaia (andesite), Tavurvur (basaltic andesite and andesite), and Sulphur Creek (andesite). These lavas are mostly restricted to the source areas although lava flows from Rabalanakaia extend to Rabaul Airport and into Greet Harbour.

Pyroclastics

Much of the geology of Rabaul is comprised of a layered sequence of relatively thin pyroclastic units,

mainly ignimbrite and airfall tephra. The sequence is complicated by erosional unconformities and by large spatial variations in thickness of individual units due to locally deep dissection of successive inter-eruption surfaces. The older pyroclastics are nearly flat-lying, and in many localities are unconformably mantled by a veneer of the youngest ignimbrites (Fig. 7). In the absence of a detailed chronology for the various pyroclastics, the most likely age for the major unconformity between the "older" and "younger" pyroclastics is taken to be about 18,000 yrs BP. This was the time of the last glacial maximum when sea level was more than 80 m below present level (Bloom et al., 1974), probably at -130 m (Chappell and Shackleton, 1986), and the lower base level would have accentuated the erosion which occurred through the present sea level altitude.

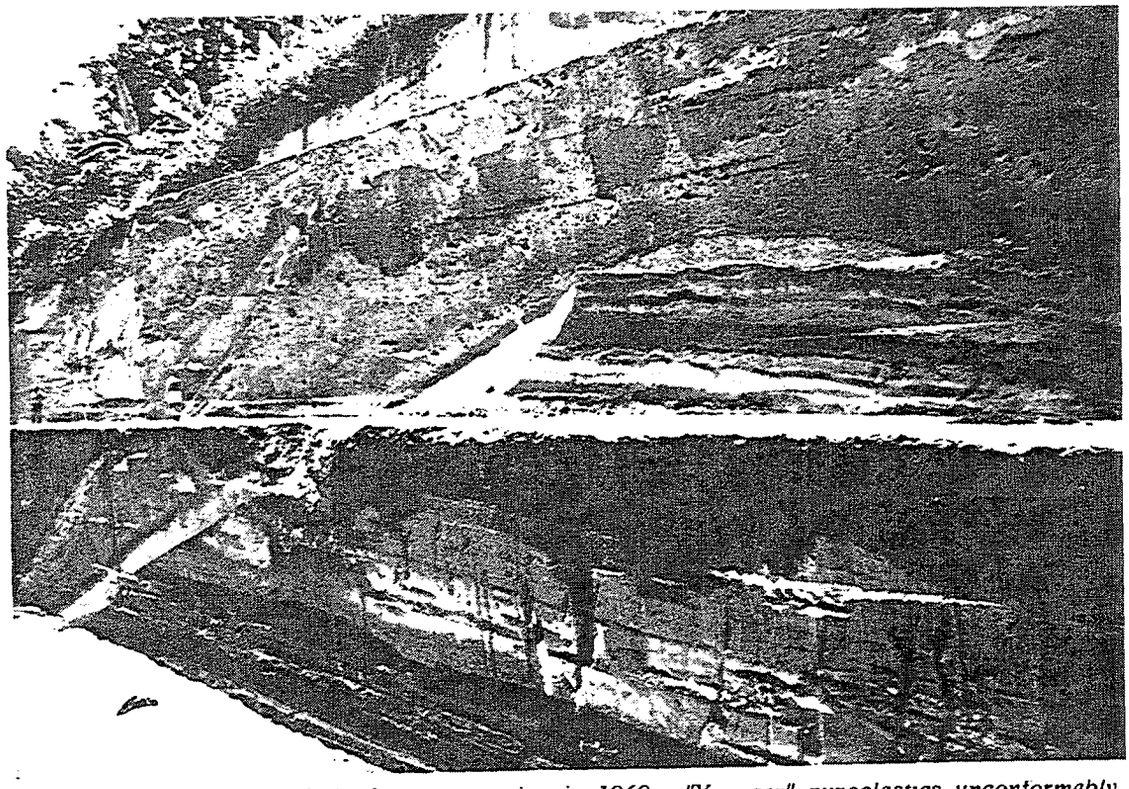

*Fig. 7. Kabakada road cutting following construction in 1969. "Younger" pyroclastics unconformably overlie nearly flat-lying "Older" pyroclastics, here represented by the Kabakada Subgroup. Photo by R.F. Heming.*

The pyroclastic deposits at Rabaul include ignimbrites, surge deposits, welded and unwelded scorias, plinian pumice beds, ash deposits, and fine grained vitric ashes. Ignimbrites make up the bulk of the volume of pyroclastic deposits. Details of these deposits follow.

*(i) Ignimbrites*

Ignimbrites at Rabaul have been of both low and higher aspect ratio types (Walker et al., 1980; Walker, 1983). The youngest, the 1400 yrs BP. Rabaul Ignimbrite is a type example of low aspect ratio ignimbrite, having been generated in an extremely violent, energetic and damaging eruption presumably by collapse of a high plinian eruption column. This ignimbrite travelled distances of at least 50 km forming a sheet-like deposit. In palaeovalleys it ponded to thicknesses of 30-40 m while on interfluves it is represented as thin veneer deposits. Its volume has been estimated to be about 8 $km^3$. A full description of the Rabaul Ignimbrite and associated deposits and their eruption mechanisms is given by Walker et al. (1981). Most of the older ignimbrites appear to be of higher aspect ratio.

Compositional zoning or variation within ignimbrites at Rabaul is rare. However, one of the pyroclastic units, the Malaguna Pyroclastics whose age is c. 0.11 Ma, provides an interesting example of compositional variation. The basal part of this unit is a pale grey plinian deposit of rhyodacitic composition (Fig. 8). Overlying this is a zone of dark grey andesitic welded ignimbrite. This in turn grades into an unwelded ignimbrite containing mixed brown and grey pumices whose compositions are andesitic and dacitic respectively.

Most of the ignimbrites at Rabaul are low grade (Walker, 1983) or unwelded. In the case of the Rabaul Ignimbrite the magmatic quench temperature was high at 835-1035°C (Heming and Carmichael, 1973), but the deposit is virtually unwelded. The lack of welding in this ignimbrite, and other Rabaul-sourced ignimbrites, could be due to some cooling by ingestion of sea water (Nairn et al., 1989). One notable exception is the Latlat Pyroclastics formation. Near its presumed source in the southwestern part of the caldera

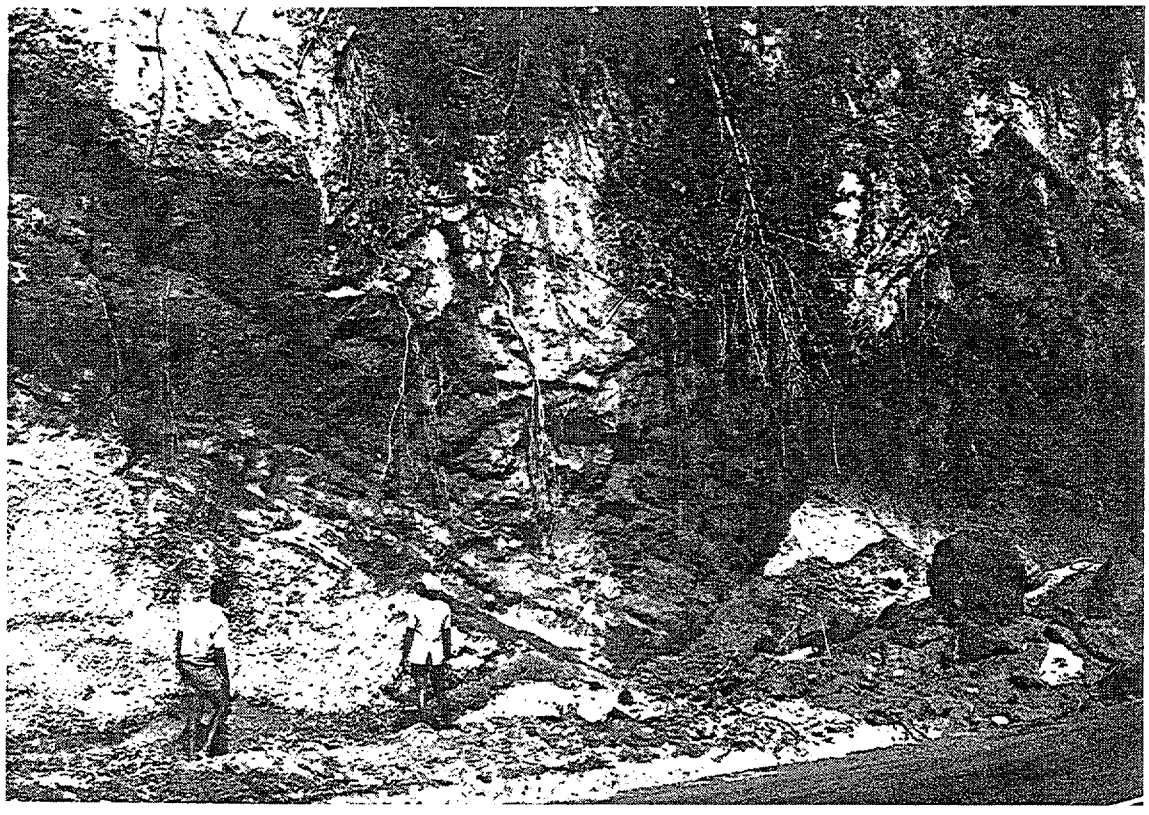

*Fig. 8. Compositional variation within the Malaguna Pyroclastics. The pale-coloured Plinian pumice basal unit is rhyodacitic while the overlying dark welded unit is andesitic. This in turn grades into a pale unwelded ignimbrite containing mixed brown and grey pumices whose compositions are andesitic and dacitic respectively. Photo by I.A. Nairn.*

welding ccupies a zone several tens of metres thick. The degree of welding varies greatly from moderately welded zones in which vitric chips and shards are lightly compressed and tack-welded together, to zones of intensely welded dark glass.

*(ii) Plinian deposits*

Associated with nearly all of the ignimbrites at Rabaul are Plinian pumice beds. Clasts in these deposits are typically highly vesiculated (Fig. 9). In most cases these deposits are less than 1 m thick. However, the Plinian layer at the base of the Malaguna Pyroclastics is as much as 10 m thick in some exposures.

Grading, both normal and reversed, is present in the Plinian deposits. A few of the Plinian deposits show alternating bands of coarse and fine pumice and ash. This has been attributed to rain-flushing in the eruption plume (Walker et al., 1981). Another possible explanation for this feature is that conditions at the vent may have alternated between wet and dry as sea or lake water occasionally accessed the vent.

At distal exposures many of the ignimbrites are missing or are very thin, while their associated Plinian deposits are proportionally thicker.

*(iii) Welded and unwelded scorias*

Scoria deposits make up a significant proportion of the cones Kombiu, Palangiagia and Turangunan but few are widely distributed. Those that form sheet-like deposits are the Karavia Welded Tuff and the Scoria Fall unit of the Raluan Pyroclastics.

The Karavia Welded Tuff includes the oldest exposed scoria deposit at Rabaul. It comprises a sequence of interbedded grey tack-welded coarse fall deposits and black densely welded crystal-vitric tuffs with platy jointing. It is characterized by abundant included lithic clasts. In an exposure at the base of the western wall of the caldera it is more than 30 m thick. The intensity of welding varies considerably within the unit. In places, sintered sand to gravel-sized crystal and lithic debris are roughly bedded on a mm to cm scale with black glass lenses. Densely welded platy tuff retains vitroclastic texture though shards are flattened, stretched and contorted, and in places flow has occurred. The essential material in this deposit is of dacitic composition.

The youngest widespread scoria deposit is the airfall scoria unit at the base of the Raluan Pyroclastics (erupted c. 6800 yrs BP.). This unit is unwelded and was distributed mainly to the west of the caldera. Its composition is basaltic, contrasting markedly with the directly overlying rhyolitic ignimbrite unit of the Raluan Pyroclastics. The sub-Plinian dispersal of the scoria may be a consequence of the bi-modal character of the Raluan Pyroclastics where volatiles from the rhyolite could have boosted the intensity of the eruption of the scoria.

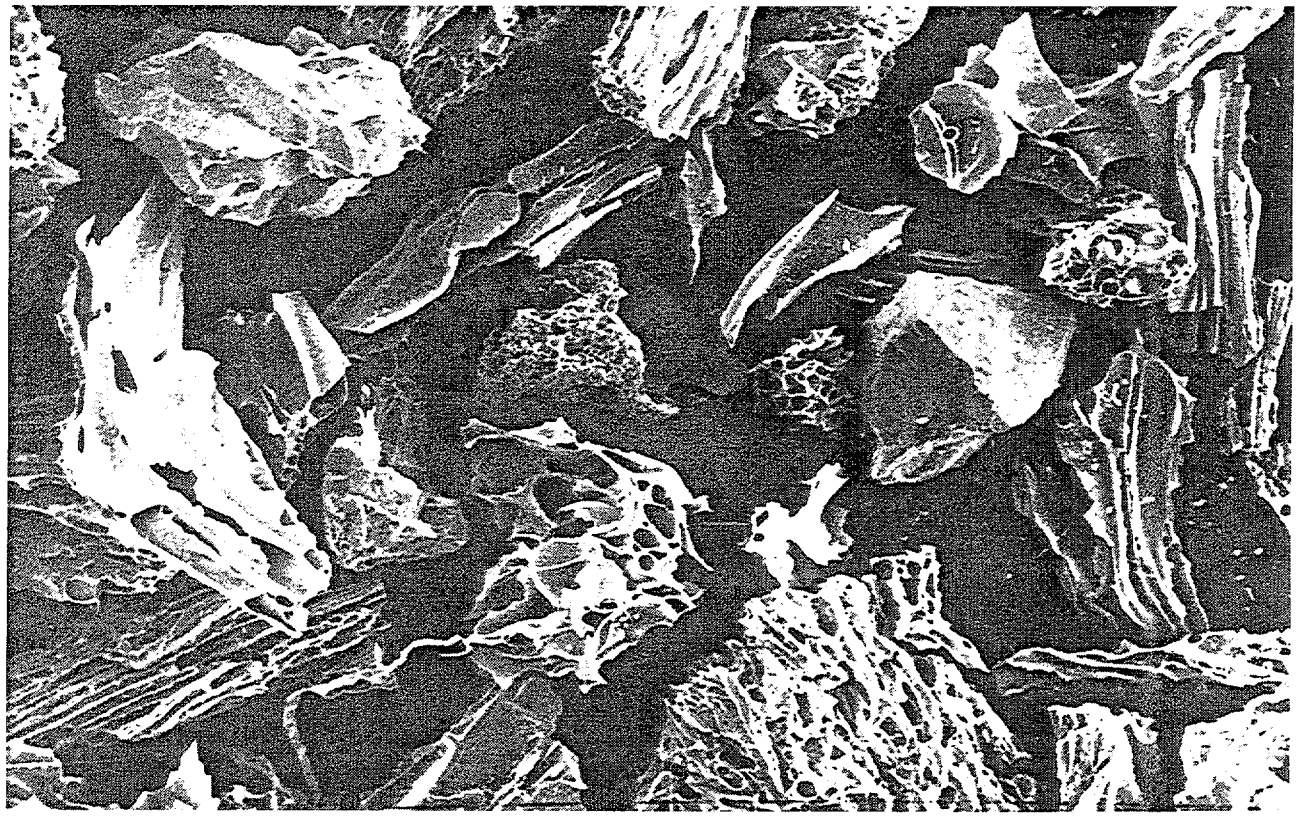

*Fig. 9. Scanning electron microscope (SEM) image of highly vesiculated pumice clasts from the 63-250 micron size fraction of a Plinian pumice deposit at Kabakada. Scale bar = 100 microns. Image by I.A. Nairn.*

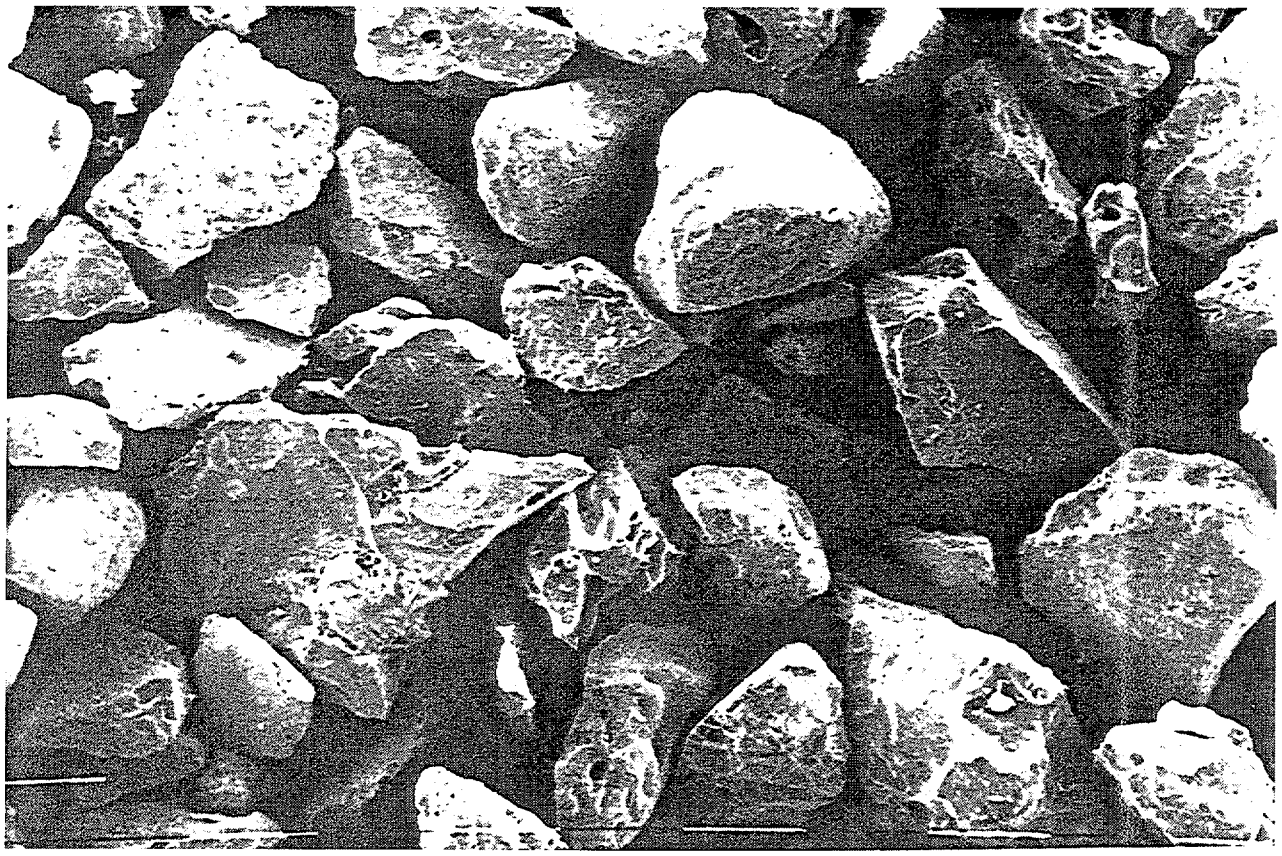

*Fig. 10. Scanning electron microscope (SEM) image of angular, fracture-bounded, dense clasts from the 63-250 micron size fraction of a fine grained vitric ash (FGVA) at Kabakada. Scale bar = 100 microns Image by I.A. Nairn.*

*(iv) Fine grained vitric ashes*

There are many fine grained vitric ash (FGVA) deposits in the Rabaul pyroclastic sequence. Typically, these deposits are mid-dark grey in colour and appear mafic, but in fact are dacitic in composition. The submillimetre size fraction usually exceeds 95 wt %. The FGVA are comprised mostly of angular, non- to slightly-vesicular brown-grey essential vitric clasts having arcuate fracture-bounded, smooth surfaces (Fig. 10). Crystals show "chatter mark" step fracture surfaces. The clast morphology indicates explosive magma-water interaction (Sheridan and Wohletz, 1983; Wohletz, 1983), probably as a result of chilling and frittering of a dacitic magma body on entry into shallow water.

The FGVA usually directly underlie and in some cases are interbedded with Plinian pumice deposits. These relationships are interpreted as demonstrating an initial "wet" phreatomagmatic style of eruption which later changed to a typical "dry" Plinian pumice eruption mode. Associated FGVA and Plinian pumice beds are mineralogically similar but show small chemical variations. This suggests that two vents were sequentially or simultaneously active, tapping a zoned magma body.

Although most common in the upper Rabaul stratigraphy, FGVA deposits occur throughout the pyroclastic sequence. The FGVA lithology is significant in demonstrating the presence of abundant external water during eruptions and thus the probable existence of caldera lakes (or bays) from an early stage of Rabaul eruption history.

Sediments

The only sediments mapped at Rabaul are the Tavui Limestones and the Matupit Pumice Sediments. The Tavui Limestones are uplifted coral and shell reef limestones which outcrop in the Tavui Point area to the north of Rabaul. The upper surface of the limestone is as much as 40 m a.s.l. at Tavui Point - here the base is near current sea level. These rocks are interbedded with pyroclastics. The Tavui Limestones are rich in coral, mollusca, and foraminifera of Pleistocene age including many foraminifera species found in present-day reefs (Fisher, 1939).

The limestones at Tavui underlie the Malaguna Pyroclastics (the age of which is c. 0.11 Ma). From nannofossil data, the silts directly beneath the Tavui Limestones are indicated to have been deposited between 85 ka and 268 ka. Because eustatic sea levels have been lower than present except during the last interglacial at about 125 ka (Bloom et al., 1974; Chappell and Shackleton, 1986), this is considered to be the most likely age for the uplifted limestone. Other times of sea level maxima did not reach such high levels and seem less likely to correlate with the limestone as more rapid rates of uplift would be required to raise the limestone from these low levels to the present position.

The Matupit Pumice Sediments are water-sorted, sea-rafted dacitic pumice lapilli and ash beds exposed in uplifted coastal exposures at Matupit Island and Sulphur Point. These sediments are directly overlain by beach deposits and are exposed only where uplifted above sea level, but have been identified in off-shore sediment cores and are probably present over most of the caldera floor. Their source is thought to be the vent associated with the Dawapia Rocks.

These pumiceous sediments are stratified into poorly-sorted ash-dominated, and better-sorted lapilli/block dominated parallel bedded layers. However, the ash-dominated beds show low-angle cross-bedding. The coarse layers are commonly reverse graded. Both light and dark pumice are present, as well as banded pumice. Rare dense lithic blocks are present but have no underlying impact sags. The base of the Matupit Pumice Sediments is not exposed and the greatest thickness above sea level is about 17 m.

Shell and coral samples from the beach deposits overlying the Matupit Pumice Sediments have given $^{14}C$ dates which average at about 750 yrs BP.

## PETROLOGY

The volcanic rocks at Rabaul constitute a medium-K to high-K calc-alkaline series (Fig. 11). The most primitive rocks are olivine-bearing high-alumina basalts. These basaltic lavas are the origin for a continuous calc-alkaline trend through basaltic andesite, andesite, dacite to rhyodacite. The only rhyolite analyses are from the 6,800 yrs BP. Raluan Ignimbrite which is clearly unrelated to the high-K trending volcanics (Fig. 11). Major and trace element data for a selection of Rabaul rocks are given in Table 1. Rock sample identifications and locality details are given in Table 2.

The high-alumina basalts are generally porphyritic having phenocrysts of calcic plagioclase, augite, magnesian hypersthene, olivine and titanomagnetite. Basaltic andesite has a similar mineralogy to high-alumina basalt, except that olivine is less abundant, and orthopyroxene more common. The mineralogy of the andesites and dacites is very similar. They contain phenocrysts and microlites of plagioclase (andesine-labradorite), hypersthene, augite, Fe-Ti oxides (magnetite predominant over ilmenite), and accessory apatite. The mineralogy of the Raluan Pyroclastics rhyolite includes all of the phases seen in the dacites but in addition has common quartz phenocrysts and rare hornblende.

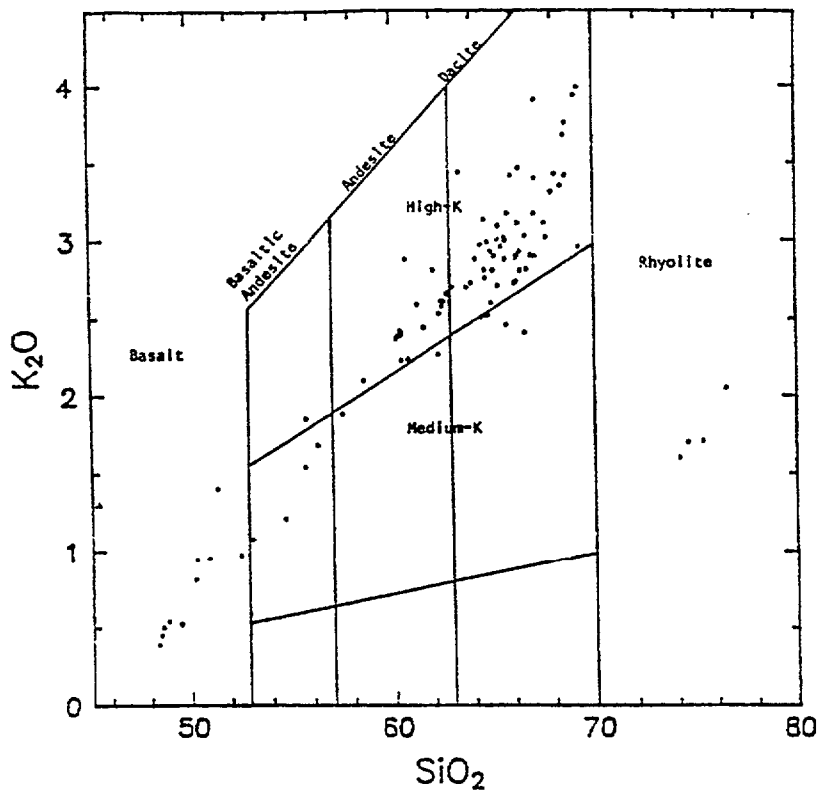


*Fig. 11. Variation of $K_2$ and $SiO_2$ (after Nairn et al., 1989). Grid is from Gill (1981) extended into the dacite field.*

Geochemistry of the Rabaul rocks shows a number of clear trends. For major elements in the basalt-rhyodacite sequence, $SiO_2$ has strong positive correlation with $Na_2O$ and $K_2O$ and very strong negative correlation with $Al_2O_3$, $Fe_2O_3$, MgO and CaO (Fig. 12). Trace element variations against silica show strong negative correlations for V, Sr, Cr and Ni, and strong positive correlations for Rb, Y, Zr, Ba, and rare earth elements (Fig. 13). Between rhyodacite and rhyolite there are clear breaks in the trends for many of the major and trace element variations against silica, though the $K_2O$ vs $SiO_2$ variation (Fig. 11) most clearly shows the rhyolite to be unequivocally different from the basalt-rhyodacite trend.

The AFM (Alkali-Fe-Mg) diagram (Fig. 14) has a typically calc-alkaline trend, showing no iron enrichment. However, comparison with the field of high-K orogenic volcanics from the Western Pacific (Ewart, 1982) shows that rocks at the low-alkali end of the Rabaul trend are enriched in iron. The rhyolite of the Raluan Pyroclastics lies at the extreme alkali-rich end of the AFM trend, despite its low $K_2O$ content. Two analyses of the Malaguna Pyroclastics Plinian pumice plot with the rhyolite analyses, which are otherwise clearly separated from the high-K dacites.

Crystal fractionation has been shown (Heming, 1974; Nairn et al., 1989) to be a feasible process for a line of descent from basalt to rhyodacite at Rabaul. The parent basaltic composition is presumed to be derived from subduction zone partial melts. A smooth progression from high-alumina basalt to the most siliceous dacite can be modelled. Even large compositional differences between analysed samples can be successfully modelled. This is so in the case of the compositionally zoned Malaguna Pyroclastics where eruption commenced with rhyodacite which was closely followed by andesite with which it mixed to produce banded pumice and possibly the dacitic products that constitute the bulk of the formation. The direct step from the andesite to the rhyodacite of the Malaguna Pyroclastics can be modelled quite successfully.

Crystal fractionation is clearly not the sole process responsible for the observed suite of compositions ranging from high-alumina basalt to high-K dacite. Mixing of magmas is evident in the products of several eruptions, notably the Malaguna Pyroclastics, and other processes may also be involved in the generation of different magmas. However, the bulk of the Rabaul rocks show consistent petrographic and chemical trends suggesting that similar physical conditions have prevailed during the evolution and eruption of most of the Rabaul magmas. There is no clear trend in composition with time. Basalts, andesites and dacites

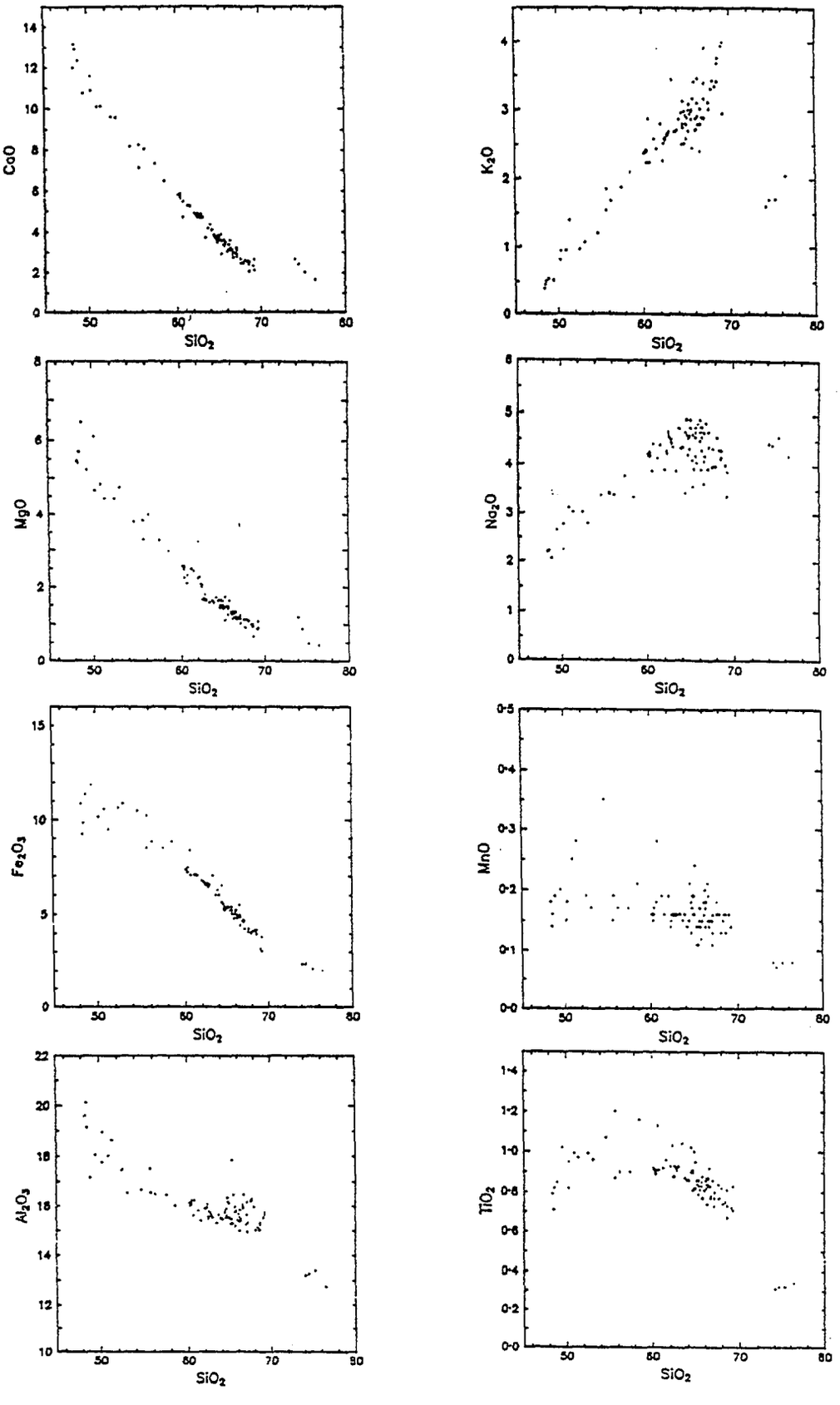


*Fig. 12. Major element variation against $SiO_2$ for Rabaul volcanic rocks (after Nairn et al., 1989).*

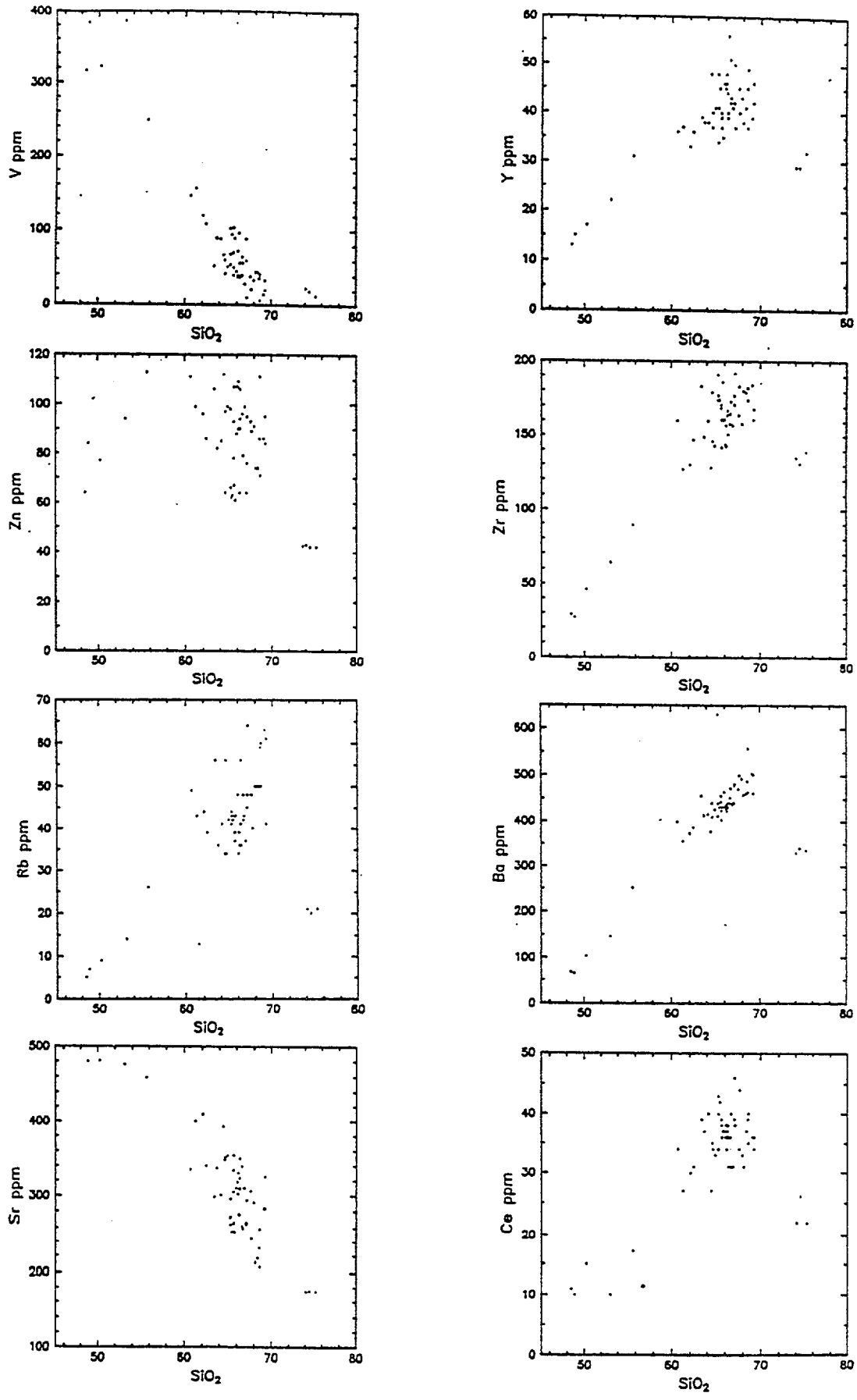


*Fig. 13. Trace element variation against $SiO_2$ for Rabaul volcanic rocks (after Nairn et al., 1989).*

*Table 1. Major and trace element chemical analyses of selected volcanic rocks from the Rabaul area. Trace elements are in ppm, and are denoted by - if not analysed. The list is sorted according to $SiO_2$* (see subnote). See Table 2 for sample identifications and locality details.*

| | 1 | 2 | 3 | 4 | 5 | 6 | 7 | 8 | 9 | 10 |
|---|---|---|---|---|---|---|---|---|---|---|
| $SiO_2$ | 48.85 | 50.05 | 55.99 | 59.55 | 60.74 | 62.51 | 62.19 | 63.42 | 62.02 | 64.71 |
| $TiO_2$ | 0.72 | 0.82 | 0.90 | 1.11 | 0.91 | 0.92 | 0.91 | 0.87 | 0.87 | 0.81 |
| $Al_2O_3$ | 20.27 | 17.70 | 16.41 | 15.34 | 15.56 | 15.64 | 15.48 | 15.57 | 15.21 | 15.93 |
| $Fe_2O_3$# | 9.29 | 10.14 | 8.79 | 8.21 | 6.62 | 6.58 | 6.51 | 6.00 | 5.44 | 5.29 |
| MnO | 0.14 | 0.15 | 0.17 | 0.18 | 0.19 | 0.16 | 0.16 | 0.15 | 0.20 | 0.13 |
| MgO | 5.44 | 6.08 | 3.97 | 2.07 | 2.18 | 1.67 | 1.63 | 1.63 | 1.58 | 1.44 |
| CaO | 13.25 | 11.55 | 8.02 | 4.65 | 4.80 | 4.70 | 4.71 | 4.19 | 3.69 | 3.83 |
| $Na_2O$ | 2.22 | 2.22 | 3.36 | 3.81 | 3.83 | 4.43 | 4.47 | 4.70 | 4.48 | 4.60 |
| $K_2O$ | 0.45 | 0.81 | 1.67 | 2.83 | 2.75 | 2.65 | 2.64 | 2.69 | 2.42 | 3.14 |
| $P_2O_5$ | 0.12 | 0.13 | 0.26 | 0.39 | 0.29 | 0.36 | 0.35 | 0.36 | 0.34 | 0.31 |
| LOI | -0.53 | -0.60 | 0.15 | 1.40 | 1.41 | 0.35 | 0.63 | 0.00 | 3.48 | 0.01 |
| Total | 100.22 | 99.05 | 99.69 | 99.54 | 99.28 | 99.97 | 99.68 | 99.58 | 99.73 | 100.20 |
| | | | | | | | | | | |
| $SiO_2$* | 48.49 | 50.23 | 56.25 | 60.68 | 62.06 | 62.75 | 62.79 | 63.69 | 64.44 | 64.59 |
| $K_2O$* | 0.45 | 0.81 | 1.68 | 2.88 | 2.81 | 2.66 | 2.67 | 2.70 | 2.51 | 3.13 |
| | | | | | | | | | | |
| V | 316 | 322 | - | 146 | 119 | - | - | 89 | 67 | 60 |
| Cr | 25 | 28 | - | <5 | <5 | - | - | <5 | 4 | <5 |
| Ni | 24 | 30 | - | <5 | <5 | - | - | <5 | 3 | 5 |
| Zn | 64 | 77 | - | 111 | 96 | - | - | 82 | 112 | 64 |
| Ga | 17 | 16 | - | 16 | 17 | - | - | 17 | 21 | 17 |
| Rb | 5 | 9 | - | 49 | 44 | - | - | 36 | 34 | 56 |
| Sr | 543 | 481 | - | 335 | 410 | - | - | 337 | 393 | 348 |
| Y | 13 | 17 | - | 36 | 33 | - | - | 38 | 48 | 37 |
| Zr | 29 | 46 | - | 160 | 130 | - | - | 149 | 128 | 179 |
| Nb | <5 | <5 | - | <5 | <5 | - | - | <5 | 7 | <5 |
| Ba | 68 | 103 | - | 398 | 373 | - | - | 413 | 377 | 440 |
| La | 2 | <2 | - | 14 | 12 | - | - | 12 | 13 | 15 |
| Ce | 11 | 15 | - | 34 | 30 | - | - | 37 | 27 | 35 |
| Nd | <10 | <10 | - | 20 | 19 | - | - | 25 | 20 | 27 |
| Pb | 4 | 5 | - | 14 | 12 | - | - | 10 | 8 | 11 |

*Table 1 (continued)*

| | 11 | 12 | 13 | 14 | 15 | 16 | 17 | 18 | 19 | 20 |
|---|---|---|---|---|---|---|---|---|---|---|
| $SiO_2$ | 62.35 | 63.43 | 65.64 | 64.43 | 64.73 | 65.52 | 65.28 | 66.24 | 66.95 | 73.11 |
| $TiO_2$ | 0.91 | 0.77 | 0.83 | 0.79 | 0.80 | 0.82 | 0.71 | 0.69 | 0.80 | 0.31 |
| $Al_2O_3$ | 14.92 | 15.04 | 15.38 | 15.05 | 15.03 | 15.22 | 14.39 | 14.88 | 15.13 | 13.04 |
| $Fe_2O_3$# | 5.19 | 5.27 | 5.43 | 4.68 | 5.04 | 4.91 | 3.96 | 3.06 | 3.71 | 2.34 |
| MnO | 0.18 | 0.11 | 0.14 | 0.15 | 0.16 | 0.17 | 0.12 | 0.15 | 0.14 | 0.08 |
| MgO | 1.57 | 1.69 | 1.48 | 1.29 | 1.26 | 1.29 | 1.04 | 0.84 | 1.04 | 1.18 |
| CaO | 3.71 | 3.79 | 3.60 | 2.97 | 3.34 | 3.20 | 2.50 | 2.23 | 2.57 | 2.62 |
| $Na_2O$ | 4.40 | 3.99 | 4.62 | 4.69 | 4.38 | 4.49 | 4.35 | 3.83 | 3.25 | 4.36 |
| $K_2O$ | 2.50 | 2.93 | 3.11 | 3.34 | 2.83 | 2.89 | 3.29 | 3.78 | 2.86 | 1.58 |
| $P_2O_5$ | 0.32 | 0.19 | 0.28 | 0.27 | 0.27 | 0.24 | 0.18 | 0.15 | 0.22 | 0.06 |
| LOI | 3.56$ | 2.97 | -0.19 | 2.14 | 1.75 | 1.41 | 3.98 | 3.73 | 3.62 | 1.41 |
| Total | 99.61 | 100.18 | 100.32 | 99.80 | 99.59 | 100.16 | 99.80 | 99.58 | 100.29 | 100.09 |
| | | | | | | | | | | |
| $SiO_2$* | 64.91 | 65.25 | 65.31 | 65.97 | 66.16 | 66.35 | 68.13 | 69.11 | 69.26 | 74.09 |
| $K_2O$* | 2.60 | 3.01 | 3.09 | 3.42 | 2.89 | 2.93 | 3.43 | 3.94 | 2.96 | 1.60 |
| | | | | | | | | | | |
| V | - | 102 | 68 | 45 | 72 | 38 | 44 | 14 | 33 | 23 |
| Cr | - | <5 | <5 | 1 | 3 | <5 | <5 | <5 | 3 | <5 |
| Ni | - | 11 | 5 | 4 | 3 | <5 | <5 | <5 | 2 | <5 |
| Zn | - | 66 | 62 | 88 | 90 | 94 | 74 | 86 | 95 | 43 |
| Ga | - | 16 | 17 | 16 | 15 | 17 | 15 | 15 | 17 | 12 |
| Rb | - | 41 | 43 | 48 | 39 | 41 | 50 | 63 | 41 | 21 |
| Sr | - | 273 | 296 | 310 | 302 | 323 | 212 | 283 | 325 | 174 |
| Y | - | 34 | 41 | 46 | 46 | 39 | 38 | 39 | 46 | 29 |
| Zr | - | 174 | 177 | 161 | 157 | 167 | 180 | 184 | 161 | 135 |
| Nb | - | <5 | <5 | 8 | 8 | <5 | <5 | 7 | 6 | <5 |
| Ba | - | 412 | 440 | 464 | 436 | 440 | 458 | 503 | 461 | 329 |
| La | - | 12 | 16 | 14 | 16 | 17 | 16 | 16 | 15 | 9 |
| Ce | - | 34 | 40 | 37 | 38 | 38 | 31 | 36 | 34 | 22 |
| Nd | - | 27 | 24 | 24 | 21 | 26 | 26 | 27 | 22 | 16 |
| Pb | - | 10 | 9 | 11 | 10 | 12 | 12 | 13 | 11 | 8 |

*Subnote:*
*$Fe_2O_3$# is total Fe expressed as ferric oxide.*
*LOI is loss-on-ignition, for all samples except the one from Heming and Carmichael (1973), and Heming (1974) (denoted by $_{\$}$) which is combined $H_2O^-$ and $H_2O^+$.*
*$SiO_2$* and $K_2O$* are the values after the analysis has been calculated to 100% on LOI-free or Water-free basis; these values have been used to chemically classify the samples.*

*Table 2. Identification and locality details of the rock samples whose chemical analyses are given in Table 1. The second column gives the grid reference (where known) on 1:50,000 map sheets 6245 III and IV and 6244 IV. Text gives stratigraphic correlation, chemical classification, a brief description of sample lithology (where known), and locality.*

| | | |
|---|---|---|
| 1. | 098345 | Palangiagia Lavas. High-Alumina Basalt. Lava flow, Palangiagia . |
| 2. | 041315 | Raluan Pyroclastics Scoria Fall Member. High-Alumina Basalt. Scoria in cutting, Burma Road. |
| 3. | - | Tavurvur Lavas. Basaltic Andesite. Lava flow in wall of explosion crater S flank, Tavurvur. |
| 4. | 995351 | Vunairoto Lapilli. High-K Andesite. Dark lapilli in fine grey ash, Kabakada reference section road cutting. |
| 5. | 065360 | Malaguna Pyroclastics. High-K Andesite. Welded tuff, Tunnel Hill cutting. |
| 6. | - | Vulcan 1937 Pyroclastics. High-K Andesite. Glassy exterior of a bomb. Vulcan. |
| 7. | - | Vulcan 1878 Pyroclastics. High-K Andesite. Dense glassy exterior of a bomb. Vulcan. |
| 8. | 122313 | Tavurvur 1937-43 Pyroclastics. High-K Dacite. Block ejected in 1941-43 eruptions, Tavurvur summit. |
| 9. | 995351 | Kulau Ignimbrite. Dacite. Pumice from ignimbrite, in Kabakada reference section road cutting. |
| 10. | 098362 | Rabaul Quarry Lavas. High-K Dacite. Lava in caldera wall, Rabaul Quarry. |
| 11. | - | Rabaul Pyroclastics Formation, Ignimbrite Member. High-K Dacite. Pumice flow, Kabakada. |
| 12. | 007335 | Vunabugbug Pyroclastics. High-K Dacite. Plinian pumice deposit under an ignimbrite, in road cutting near Vunabugbug. |
| 13. | 109239 | Latlat Pyroclastics. High-K Dacite. Welded tuff, in road cliffs on S coast of Karavia Bay. |
| 14. | 061257 | Karavia Welded Tuffs. High-K Dacite. Welded tuff in W caldera wall near Karavia 1 village. |
| 15. | 011280 | Rabaul Pyroclastics Formation. Plinian Fall Member. High-K Dacite. Plinian pumice deposit in road cutting near Ramale. |
| 16. | 007335 | Talili Pyroclastics Subgroup. High-K Dacite. Grey vitric airfall fine ash, in a road cutting near Vunabugbug. |
| 17. | 060263 | Barge Tunnel Ignimbrite. High-K Dacite. Pumice from ignimbrite at Japanese Barge Tunnel, SW of Vulcan. |
| 18. | 065360 | Malaguna Pyroclastics. High-K Dacite. Plinian-pumice at base, Tunnel Hill cutting. |
| 19. | 061240 | Talakua Pyroclastics. High-K Dacite. Plinian pumice deposit in deep gully north of Talakua. |
| 20. | 100342 | Raluan Pyroclastics, Ignimbrite Member. Rhyolite, Pumice in gully in Palangiagia. |

have been erupted at various times throughout the known stratigraphic column, but all of the rhyodacites come from the early part of the sequence.

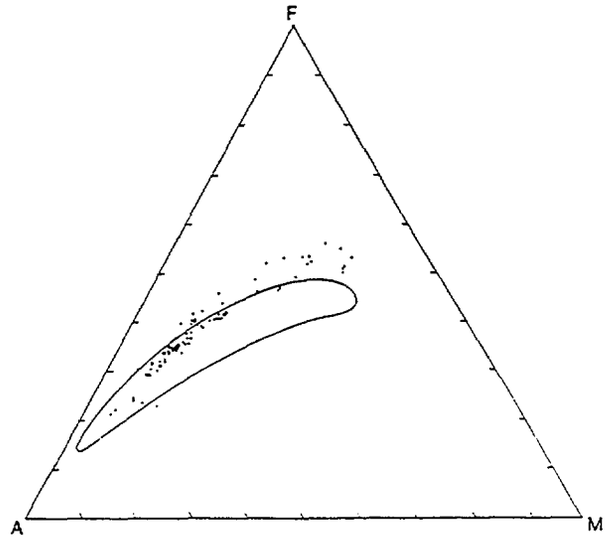


*Fig. 14. AFM plot of volcanic rocks from Rabaul (after Nairn et al., 1989). The enclosed field is the western Pacific high-K series, from Ewart (1982).*

Raluan Pyroclastics

The relationship between the rhyolite and the basalt of the Raluan Pyroclastics is somewhat enigmatic. The Raluan Rhyolite is chemically and mineralogically distinct, but is probably not unique at Rabaul. Pumice from a thin uncorrelated ignimbrite much lower in the stratigraphic sequence also contains quartz and hornblende phenocrysts and may also be rhyolitic although no chemical analyses are available. However, it is not possible to model the development of a magma of the composition of the Raluan Rhyolite from any member of the high-alumina basalt to high-K dacite suite, by fractionation of the primary minerals present in the rocks (Nairn et al., 1989). The Raluan Rhyolite has very low $K_2O$ contents (1.6 -1.7%), similar to the $K_2O$ contents of the basaltic andesites. The modelling process must start from a composition with lower $K_2O$ than that of the rhyolite. Such a starting composition would be the high-alumina basalt of the Raluan Scoria (0.81% $K_2O$) which is coeval with the rhyolite. In this case the modelled fractionation produces a rhyolite composition with anomalously high $K_2O$. Thus it is concluded that the basalt and the rhyolite of the Raluan Pyroclastics are genetically unrelated. It has been suggested that the Raluan Rhyolite was generated by partial fusion of crustal sediments (Nairn et al., 1989). Its eruption appears to have been triggered by interaction with a body of basaltic magma. Because of the physical difficulty of passing dense basaltic magma through a body of rhyolitic magma and as there is no evidence of mixing of these magmas it must be concluded that they erupted from separate vents. The basalt may have provided heat for the activation of the rhyolite.

## STRUCTURE

Structural features identified at Rabaul include large-scale regional structures, caldera margins, intra-caldera vent lineaments, and structures related to intra-caldera ground deformation (Fig. 15).

The large scale structures are tectonic faults. Many of the mapped regional faults in the area immediately south of Rabaul are oriented approximately northwest while a few trend approximately northeast, the "Warangoi Trend" (Lindley, 1988). This pattern of conjugate faulting is also evident in the fabric of smaller scale lineaments around the western and southern flanks of the caldera.

Parallel to the main northwest trend is an alignment of the major satellite cones Turangunan and Kombiu with the older volcanic centre Tovanumbatir (and possibly Watom Island). It is speculated that this alignment defines a major fracture at depth (Nairn et al., 1989).

The margin of Rabaul Caldera is defined by the scarps which surround the basin. The margin is topographically best expressed on the east as a near-vertical scarp in lavas between Turangunan and Rabalanakaia, where collapse accompanied the Rabaul Ignimbrite eruption. The collapse here was probably partially controlled by another northwest trending fracture inherited from the pre-caldera regional structure. Elsewhere the caldera scarp is usually partly buried by the Rabaul Pyroclastics and other young ignimbrite deposits, indicating that much of the present caldera rim topography predates the c. 1400 yrs BP collapse. The scalloped and eroded nature of the north, west, and south caldera scarps demonstrates that here the topographic rim represents the limit of erosional damage by slumping outwards from the true caldera ring faults lying at depth some distance inside the rim. The present caldera topography has resulted from multiple collapse events, presumably associated with each of the main ignimbrite deposits, to produce a series of nested and overlapping subsidence features. Recent seismicity (Mori et al., 1989) suggests that the presently active caldera ring fault lies within this outer structure. The seismicity defines an outward-dipping elliptical ring fault traceable to a depth of about 4 km (Fig. 19). This structure occupies the central and southern parts of the caldera. To the north, the caldera rim is older, predates the 1400 yrs BP eruption and may be related to eruption of the Raluan Pyroclastics, which

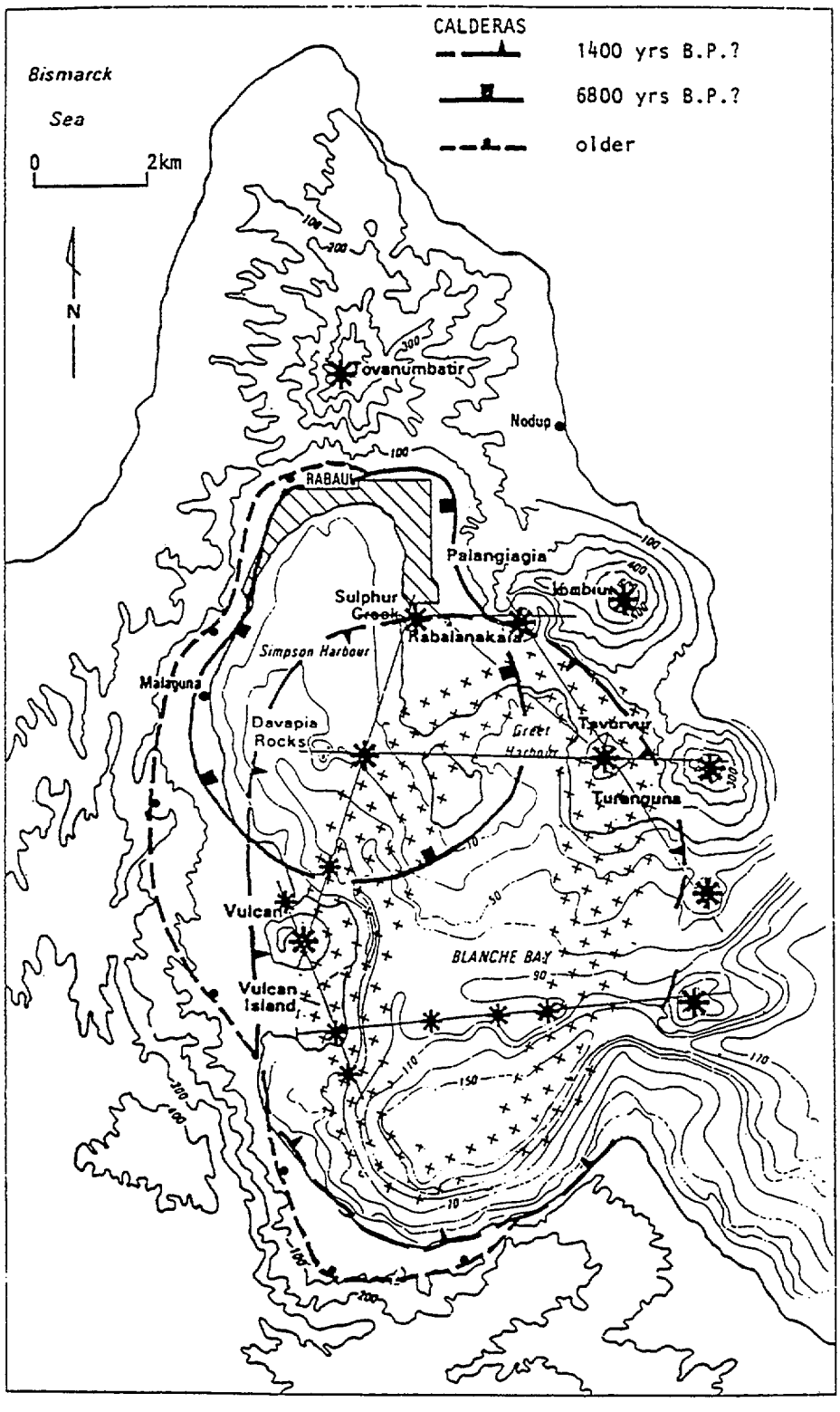


*Fig. 15. An interpretation of structures in the vicinity of Rabaul Volcano, inferred from topography, geology, vent locations, bathymetry and seismic data (after Nairn et al., 1989). Lineations defined by three or more active vents are marked. Cross-stipple marks the seismically active part of Rabaul Caldera (from Mori et al., 1989). Caldera margins shown are topographic rims.*

are thickest and coarsest on the eastern rim of this sub-caldera.

Most of the intra-caldera vents occupy positions near the edge of the presently active caldera ring fault (Fig. 15). A number of vent alignments are tangential to the ring fault. However, other vent alignments appear to transect the ring fault. The most striking of these is an east-west alignment of Vulcan Island with submarine vents in Karavia Bay, extending to a submarine prominence at the entrance to Blanche Bay. The Dawapia Rocks, Greet Harbour and Tavurvur form another east-west alignment of intra-caldera vents which, extended eastwards, includes Turangunan. A third east-west alignment is the Sulphur Creek vents with Rabalanakaia/Palangiagia and Kombiu.

A set of alignments trending north-south, is also present. The two submarine prominences at the entrance to Blanche Bay could be remnants of the caldera wall or could be discrete volcanoes, but in either case, together with Turangunan they represent a north-south lineament. Similarly, Vulcan Island/Vulcan, the Dawapia Rocks and the submarine volcanoes between them also represent a north-south lineament. In addition to the north-south alignment of these major topographic features, there is a number of fault scarps extending southwards from the southern shore of Matupit Island (Greene et al., 1986). The central one is about 2 km long. All of these features and the northerly elongation of the caldera seismic zone (Mori et al., 1986) could signify a major north-south structural trend. The inclusion of pre-caldera vents in these alignments suggests that the underlying structures may pre-date the caldera.

Episodes of both uplift and subsidence within the caldera have been reported, but the most impressive effect of intra-caldera ground deformation has been resurgence of the region between the township and Matupit Island. Uplifted beach deposits at Matupit Island and coral reefs near the Rabaul Airport are respectively about 17 m and 5 m a.s.l. The beach deposits have been dated at about 750 yrs BP while the coral has an age of about 1400 yrs BP. A total of 1.8 m of uplift was measured on Matupit Island in the period 1973-1986, and about 35% of this took place during the 1983-85 seismo-deformational crisis period (McKee et al., 1984, 1985; Mori et al., 1989). The Matupit Sediments exposed in the uplifted sea cliff on the southeast shore of Matupit Island are deformed in a small keystone-graben faulted anticline, suggestive of an underlying shallow dyke intrusion (Rubin and Pollard 1988). This graben/anticline may be related to a larger faulted anticline found offshore to the south of Matupit Island by seismic reflection profiling (Greene et al., 1986). The main source of 1973-1985 inflation in Rabaul Caldera was centred in this general area (Greene et al., 1986, McKee et al., 1985) and is inferred to result from accumulation of magma at shallow depths.

## ERUPTIVE HISTORY

### Pre-historical Activity

While a detailed stratigraphic framework has been established for Rabaul, there have been considerable problems in determining the chronology of eruptive events. Table 3 gives the eruption history of Rabaul as presently known. A K-Ar date of 0.5 Ma for a lava flow from Tovanumbatir provides a maximum age for the oldest eruptives from the Rabaul Volcano. The Rabaul pyroclastic eruptions had commenced prior to the 0.125 Ma interglacial high sea level, and were in progress at 0.11 Ma when the Malaguna Pyroclastics were erupted. The total number of ignimbrite eruptions is at least 12, and 5 of these have occurred in the last 18,000 years. Only the latest two ignimbrite eruptions have been dated confidently (1400 yrs and 6800 yrs BP). Activity at Rabaul following the 1400 yrs BP ignimbrite eruption had commenced before about 750 yrs BP.

### Historical Activity

1767 Ash emission was reported, presumably from Tavurvur but possibly from Rabalanakaia.

1791 Tavurvur emitted vast columns of black ash.

1850? Several sources report that an eruption took place in Rabaul about this time, possibly at Sulphur Creek; however, there are no eyewitness reports.

1878 At least two eyewitness reports exist of eruptions in January-February 1878 at Vulcan Island and Tavurvur. These eruptions were preceded by local changes of ground level and frequent strong local earthquakes. Initial activity took place at the site of Vulcan Island, and Tavurvur became active several hours later. Local people reported a "line of fire" or "a line of steam" linking the two eruptive centres before Tavurvur actually erupted. Vulcan Island was built up from below sea level in one night, finally reaching 3 km x 1.5 km x 20 m high. It contained a crater, breached to the sea in the southeast by a 10 m wide channel. At Tavurvur thick heavy clouds of ash were thrown out by convulsions every few minutes, along with large pumice blocks, many of which fragmented in the air. Incandescent material was thrown to 500-600 m above the crater, and a new block and ash cone was built up at the southern edge of the former crater. All vegetation within 3 km downwind (southeast) was killed. The Vulcan

*TABLE 3: Rabaul eruption history (as presently understood). Volume figures are mostly estimates. B- basalt, A- andesite, D- dacite, R- rhyolite.*

| | AGE | EVENT | MAGMA | km$^3$ |
|---|---|---|---|---|
| A.D. | 1937-43 | Tavurvur pyroclastic eruptions | A/D | 0.05 |
| | 1937 | Vulcan pyroclastic and cone-building eruptions | D/A | 0.3 |
| | 1878 | Vulcan (submarine) and Tavurvur pyroclastic eruptions | D/A | 0.3 |
| | 1850? | Sulphur Creek pyroclastic eruptions, crater forming | A | 0.1 |
| | 1791 | Tavurvur pyroclastic and lava eruptions, cone-building | A/D | 0.1 |
| | 1767 (<250 yrs by $^{14}$C) | Tavurvur? pyroclastic and lava eruptions, cone-building | A/D | 0.1 |
| | <750 yrs | Rabalanakaia pyroclastic and lava eruptions, cone-building | A | 0.2 |
| | >750 yrs | Dawapia pyroclastic eruptions, cone-building | D | 0.3 |
| | ? | Sulphur Creek lavas and pyroclastics, cone-building | A | 0.1 |
| c. | 1,400 yrs | Rabaul Pyroclastics eruptions and caldera collapse | D | >10 |
| c. | 4,400-1,400 yrs | Talili Subgroup, multiple (>7) pyroclastic eruptions producing fine vitric ashes and pumice deposits, roughly coeval with | D | 1 |
| | | Late cone-building Palangiagia Lavas, scorias | B | 0.3 |
| | | and the youngest Kombiu scorias, and | B | 0.2 |
| | | Turangunan scorias | B | 0.1 |
| c. | 6800 | Raluan Pyroclastics eruptions and caldera collapse | B,R | 5 |
| | ?-? | Talwat Subgroup, multiple (>4) pyroclastic eruptions producing fine ashes, roughly coeval with | D? | 0.5 |
| | | older cone-building Turangunan scorias and ?lava eruptions, and | B | 0.5 |
| | | Kombiu cone-building scoria and lava eruptions, and | B | 2 |
| | | Palangiagia scorias and lava eruptions, early cone-building | B | 1 |
| | <17,000 yrs | Vunabugbug Pyroclastics eruption and caldera collapse? | D | 5 |
| | | Tatoko Subgroup multiple (>4?), pyroclastic eruptions | D | 1 |
| | <17,000 yrs | Namale Pyroclastics eruption and caldera collapse? | D | 5 |
| | <18,000 yrs | Kulau Ignimbrite, major ignimbrite eruption, caldera collapse? | D | >10 |
| | >18,000 yrs | Kabakada Subgroup, multiple (>6) pyroclastic eruptions with at least 3 (small?) ignimbrites | B?,R?D | 1 |
| | >38,000 yrs | Latlat Pyroclastics | D | 5 |
| | ? | Talakua Subgroup, multiple (>7?) pyroclastic eruptions | D | 0.5 |
| c. | 40,000 yrs | Barge Tunnel Ignimbrite | D | 5 |
| | ? | Karavia Welded Scorias | D | 1 |
| | ? | Vunairoto Lapilli, pyroclastic fall | A/D | 0.1 |
| | ?-? | Tavui Subgroup, multiple (>4) pyroclastic eruptions with at least one ignimbrite | D | 0.5 |
| c. | 110,000 yrs | Malaguna Pyroclastics eruption and caldera collapse? | D/A | 5 |
| c. | 100,000 yrs | Boroi Ignimbrites | D | 10 |
| | ? | + possibly 6 more at Kerevat | D | ? |
| c. | 188 000 yrs | Rabaul Quarry Lavas | D | 0.3 |
| | ? | East Wall Lavas | D | 0.3 |
| | ? | Seismograph Lavas | B | 0.1 |
| c. | 0.5 Ma | Tovanumbatir Lavas and scoria | B | 2 |

Island centre was active for no more than a few days whereas activity at Tavurvur continued for at least two weeks. Pumice from the underwater eruption filled Blanche Bay and St George's Channel, and the harbour became so hot that turtles and fish in it were cooked .

1937 Eruptions at Vulcan and Tavurvur took place in May-June 1937 (Fisher, 1939). As in 1878, visible activity was preceded and accompanied by a series of local earthquakes and by ground deformation. Uplift of the sea-floor by as much as about 2 m was observed near Vulcan during the ten hours before eruption actually started, and perceptible earthquakes were almost continuous for about eleven hours before the commencement. A single strong shock on the preceding day is also believed to have been associated with the eruption. Eruption commenced from the western side of the caldera, and violent activity there (Fig. 16) built up the cone of Vulcan from below sea level to almost its present height (225 m) in little more than twelve hours. The column of ash and pumice reached about 8000 m high, and ash fallout was noted 150 km away, while the noise was heard about 300 km away. A number of vents on and around Vulcan were active. In contrast, the explosive eruption of Tavurvur, which commenced 21 hours after that at Vulcan, was relatively weak and produced no new material. Activity at Tavurvur took place from a northeast trending fissure which crossed the original (pre-1878) crater, and from two groups of craterlets on its outer flanks. Both eruptions were shortlived, that of Vulcan lasting about 4 days, and that of Tavurvur about 1 day. About 500 people were killed by the eruption of Vulcan, and Rabaul town and surrounding areas were damaged by pumice and ashfall (Fig. 17). Pumice from Vulcan blocked Rabaul harbour, as in 1878.

1940-43 Owing to the establishment of the Rabaul Volcanological Observatory after the 1937 eruptions, the 1941-43 eruption at Tavurvur was studied in detail and advance warnings were issued (Fisher, 1976). A few small phreatic explosions had occurred there in March 1940 without warning, but in the six months before the outbreak in June 1941, temperatures at some fumaroles increased from 99°C to 392°C and increases in the pressure and extent of the fumaroles were also noticed. This eruption was explosive, ejecting incandescent bombs and ash intermittently until March-April 1942, with a further phase in late 1943.

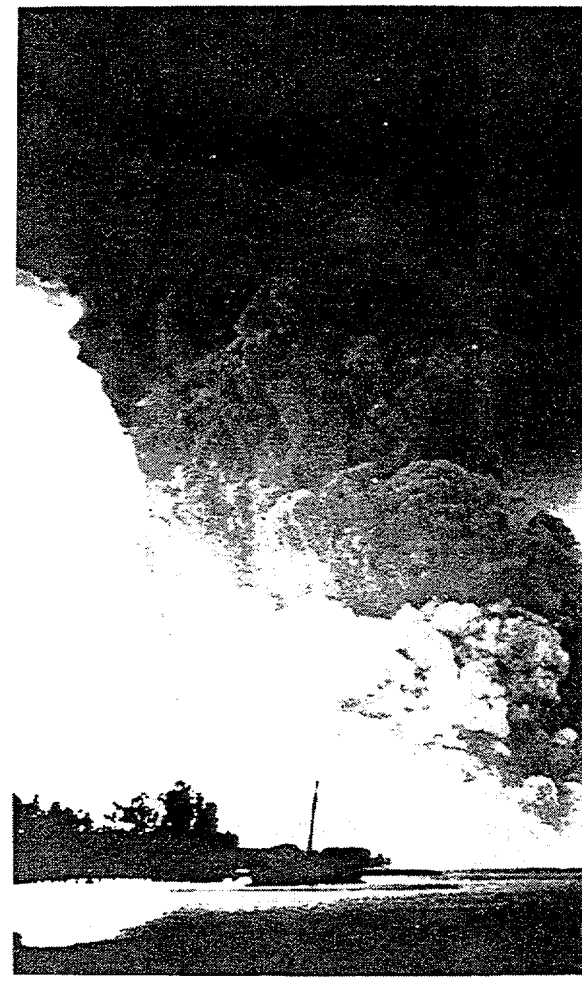

*Fig. 16. Vulcan eruption column seen from Kokopo late afternoon 29 May 1937, probably about 1 hour after the commencement of the eruption.*

## VOLCANO SURVEILLANCE

### Seismology

Seismological surveillance at Rabaul began in 1940, but it was not until 1967, when a network of seismic stations was installed around the northern part of the caldera, that a reasonable appreciation of local seismicity became possible. The seismicity of Rabaul Caldera since 1967 has consisted primarily of short-period, volcano-tectonic earthquakes originating from near surface to depths of about 6 km.

Rates of earthquake occurrence between late 1967 and late 1971 were relatively steady at between 20 and 100 earthquakes per month (Fig. 18). Higher rates of earthquake occurrence commenced in late 1971 when the first recorded swarm of caldera earthquakes took place. A general trend of progressively greater numbers of events in successive swarms was registered

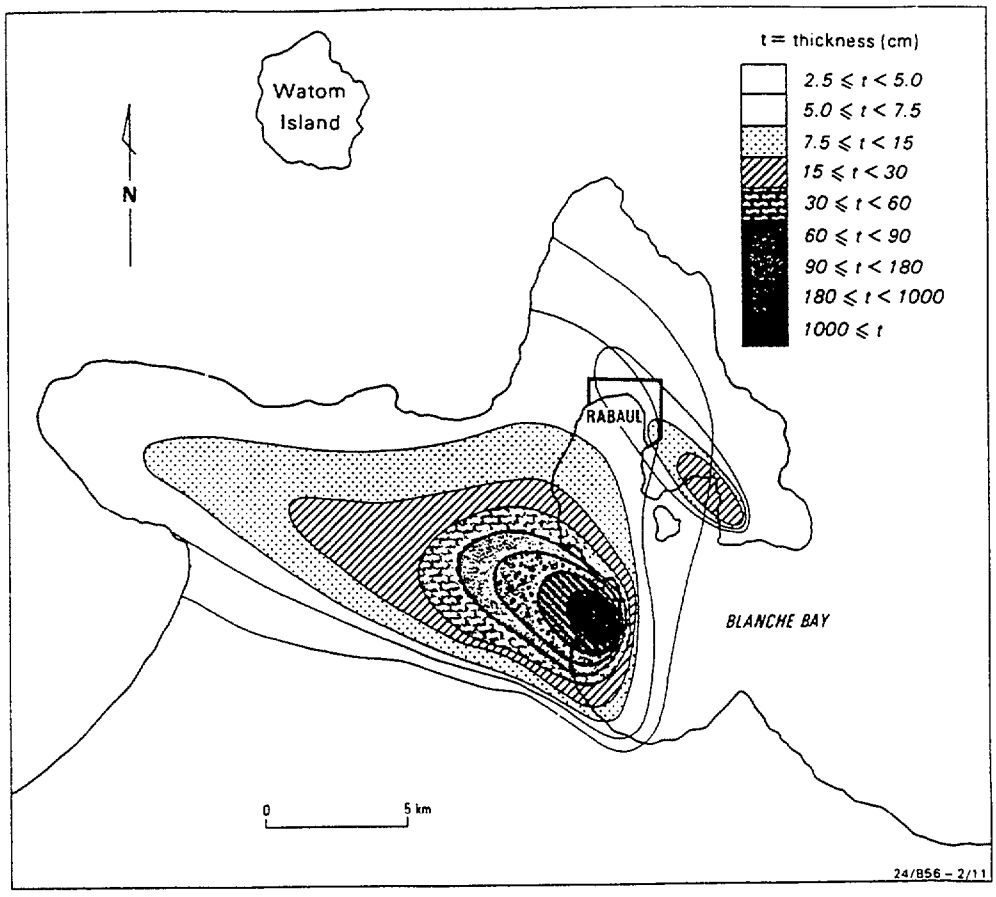


*Fig. 17. Distribution and thicknesses of tephras produced by the 1937 Vulcan and Tavurvur eruptions (adapted from Fisher, 1939). Legend refers to both the Vulcan and Tavurvur tephras, except that the outer zone for the Tavurvur tephra is for the combined range 2.5 ≤ τ ≤ 7.5.*

until 1983 when a dramatic increase in seismicity occurred. Between late 1983 and mid 1985 seismicity was markedly increased in what became known as the Seismo-Deformational Crisis Period (Mori et al., 1989). The highest monthly earthquake total during this period was almost 14,000. Since mid 1985 seismicity has fluctuated although the background has been similar to the pre-Crisis level.

The strongest caldera earthquakes have occurred during swarms. The largest magnitude event recorded so far is a $M_L$ 5.2 earthquake that occurred in October 1980. Two $M_L$ 5.1 events were recorded, in March 1982 and March 1984.

A clear picture of the seismically active parts of Rabaul Caldera has emerged. The seismicity is mostly confined to an elliptical cylindrical zone in the central-southern part of the caldera (Fig. 19). The locus of the seismicity is interpreted to be the ring fault system along which collapse took place at the time of the latest caldera-forming eruption (1400 yrs BP). Stress release related to an on-going process of inflation within the caldera is concentrated at the ring fault system. A notable feature of the ring fault/seismic zone is that in general it has an outwards dip. This is consistent with an early theoretical model of caldera formation (Anderson, 1936) but is at odds with the configuration

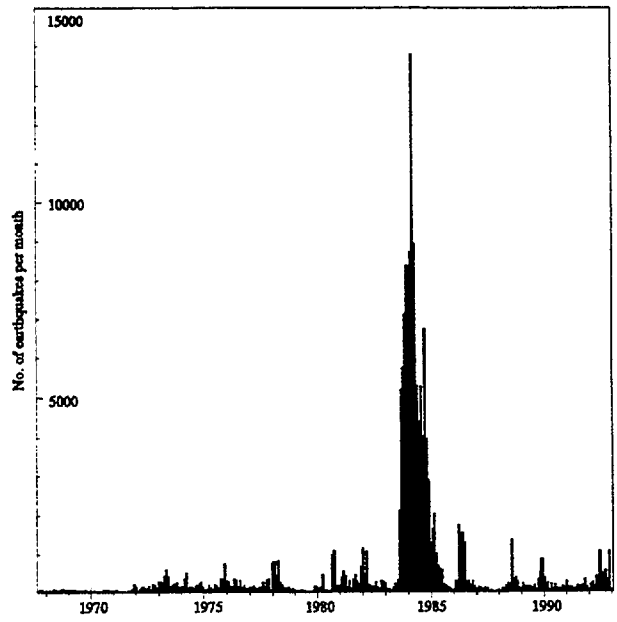


*Fig. 18. Monthly totals of Rabaul Caldera earthquakes for the period October 1967 to December 1992.*

of many other calderas and with currently preferred models of caldera formation. Fault plane solutions (Fig. 20) indicate mainly normal faulting consistent with uplift of the central part of the caldera floor and the outwards dipping ring fault. The ring fault/seismic zone at Rabaul appears not to be connected with the development of the post-caldera vents. These vents are displaced from the surface projection of the ring fault/seismic zone by 1 km or more (Mori and McKee, 1987). It is believed that the post-caldera vents occupy positions related to cone sheets developed in response to upwardly-directed magmatic pressure as in the Anderson model.

Ground Deformation

Ground deformation within Rabaul Caldera has been reported since the earliest European contacts (late-19th century) and has evidently occurred both at the times of eruptions and between them. Brown (1878) reported that at the time of the 1878 eruptions of Vulcan Island and Tavurvur, the Dawapia Rocks subsided several feet, while small rocky islets near the site of the Vulcan Island eruption were raised several feet and new rocks were exposed. At about the same time, immediately southeast of Tavurvur, the coast was uplifted about 20

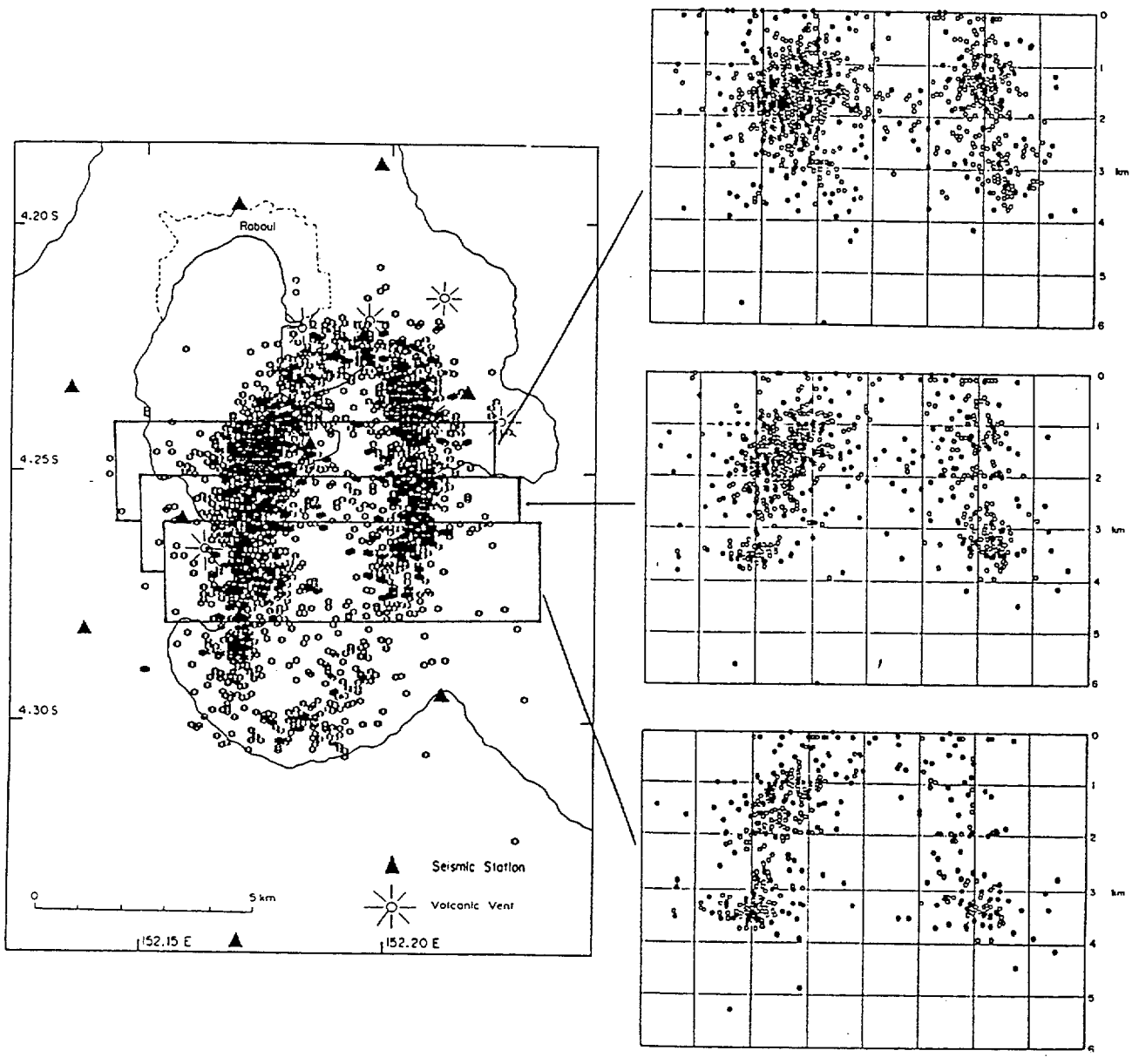


*Fig. 19. Epicentres of over 2500 earthquakes for the period September 1983 to July 1985. All earthquakes plotted were recorded on 7 or more stations and have horizontal errors of less than 1 km. In the cross sections the grid lines have a spacing of 1 km i.e. no vertical exaggeration. All events have vertical errors less than 1.5 km.*

feet and the coastline was shifted about 150 yards seawards. Several hours before the 1937 eruptions of Vulcan and Tavurvur, a number of small islets came into existence near the site of the Vulcan eruption, and a reef at the southern end of Matupit Island was exposed (Fisher, 1939). This reef subsided during or soon after the eruption as did the whole Sulphur Creek-Matupit Island-Greet Harbour area. The greatest subsidence was over 3 feet. The Dawapia Rocks also sank 3 feet or more at the time of the eruption. The deformation at the Dawapia Rocks in 1878 and 1937 and at the southeast coast of Tavurvur in 1878 has persisted to the present.

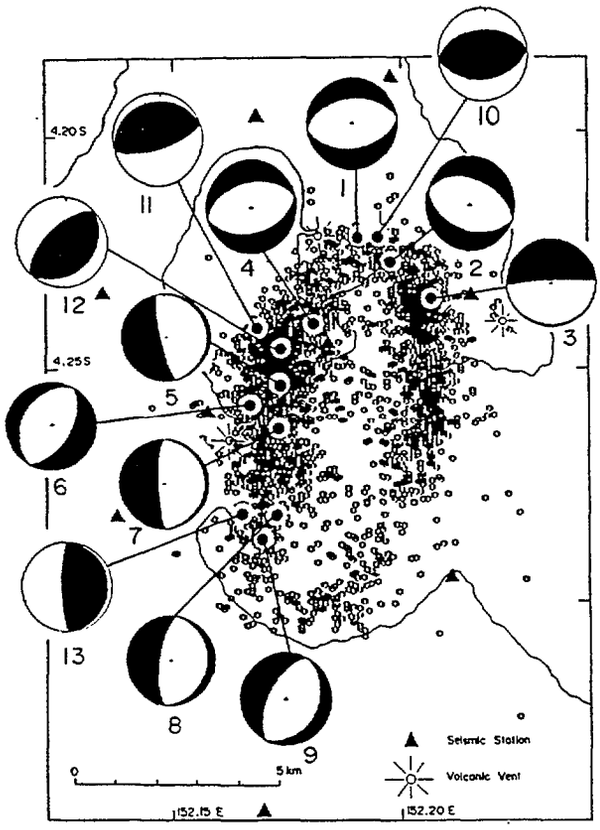


*Fig. 20 Fault plane solutions and locations of some of the larger caldera earthquakes (after Mori et al., 1989).*

Instances of deformation between eruptions were less dramatic. Uplift in the Vulcan area some years before the 1878 eruption is indicated by reports of the pre-existence there of raised coral reefs (Simpson, 1873; Schleinitz, 1889; Sapper 1910). In the two-year period before the 1941-43 eruptions of Tavurvur, subsidence of about 75 mm took place in the Greet Harbour area (Fisher, 1976).

Of particular interest is the Sulphur Creek-Matupit Island area which has a history of upheaval and subsidence between eruptions. Uplift was reported to have occurred in this area before an eruption at the head of Sulphur Creek in about 1850 (Brown, 1878), although the time scale of this uplift is not known. Fisher (1939) cited a number of instances of elevation changes in the Sulphur Creek-Matupit Island area between the 1878 and 1937 eruptions of Tavurvur and Vulcan Island/Vulcan, and small-scale topographic changes have been observed in the Sulphur Creek area since the late 1940's (Crick, 1975).

The most recent phase of deformation is an up-doming of the caldera floor. It appears that the up-doming began in late-1971 as shown by the results from tiltmeters near Sulphur Creek and Tavurvur Volcanoes (P. de Saint Ours, pers. comm., Appendix by McKee in Scott, 1982). The first indications of the scale of this up-doming came from levelling and gravity measurements in the mid-1970's. More recently, results from tilt and horizontal distance monitoring networks confirmed the trend of structural deformation and provided additional detail on the areal distribution of the deformation.

*(i) Uplift*

The pattern of deformation in Rabaul Caldera is shown best by the record of elevation changes. These changes have been monitored mainly from measurements on a levelling line extending from the northern extremity of the caldera floor to the southern end of Matupit Island. Measurements on this line commenced in August 1973, synchronously with the first gravity measurements. Surveys are usually run from a group of reasonably stable benchmarks near the northern end of this levelling line. The stability of these benchmarks is indicated by reference to sea level measurements from a tide gauge at the northern shore of Simpson Harbour which showed no significant elevation changes between 1969 and 1985 (Mori et al., 1987).

The long-term pre-Crisis uplift rate at Matupit Island was about 100 mm per year, and the maximum measured uplift between August 1973 and June 1983 was 1028 mm at the southern end of the island. The greatest measured uplift for the 23 month Crisis Period was 767 mm, at a new benchmark at the southeastern end of the island. The total measured uplift at the southern end of the Island between August 1973 and July 1985 was 1751 mm. Following the Crisis Period uplift continued to be recorded but at much lower rates than previously – about 20-30 mm per year.

Measurements on other levelling lines extending, (i) from Rabaul Town along the western and southern margins of the caldera floor and (ii) around the northern and eastern sides of Greet Harbour, have allowed the construction of a contour map of part of the deformation (Fig. 21). The main features of this deformation are a fair degree of radial symmetry and a rapid decay of uplift with distance from the source. At a distance of about 4 km the uplift is reduced to 100 mm. Other features of the deformation surface are that

it appears to be largely contained within the ring-shaped pattern of caldera seismicity (and inferred caldera ring-fault, Fig. 19), and that the focal point of the deformation is near the middle of the region bounded by the ring-fault.

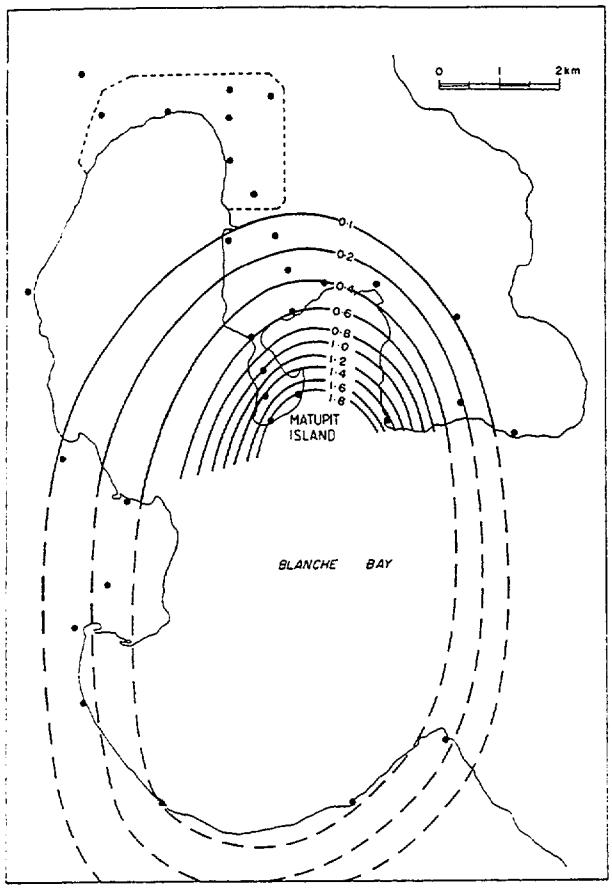


*Fig. 21. Elevation changes (m) for the period September 1973 to July 1985. Solid circles denote bench marks.*

*(ii) Tilt*

Surveillance of ground tilt in Rabaul Caldera before 1981 was limited to the measurements from four water tube tiltmeter stations, of which only two were well-situated to monitor volcanic tilt in the caldera. This network was expanded in late-1980 and early-1981 with the addition of five dry-tilt arrays.

Prior to the Crisis Period, tilt monitoring confirmed the trend of deformation which was registered by levelling measurements in the Sulphur Creek-Matupit Island area, and indicated that the source of deformation was near the mouth of Greet Harbour. Additionally, tilt measurements near Vulcan and at the southeastern shore of Karavia Bay hinted at the possibility of a second source of deformation, in the southwestern part of the caldera.

A major expansion of the network of dry tilt arrays was carried out at the beginning of the Crisis period. This allowed better resolution of the locations of the sources of deformation, particularly for the one at the mouth of Greet Harbour. The largest measured tilts in this area for the Crisis Period were almost 500 $\mu$rad while tilts of up to about 150 $\mu$rad were recorded in the Vulcan area (Fig. 22). Since the end of the Crisis Period rates of tilting have been very low.

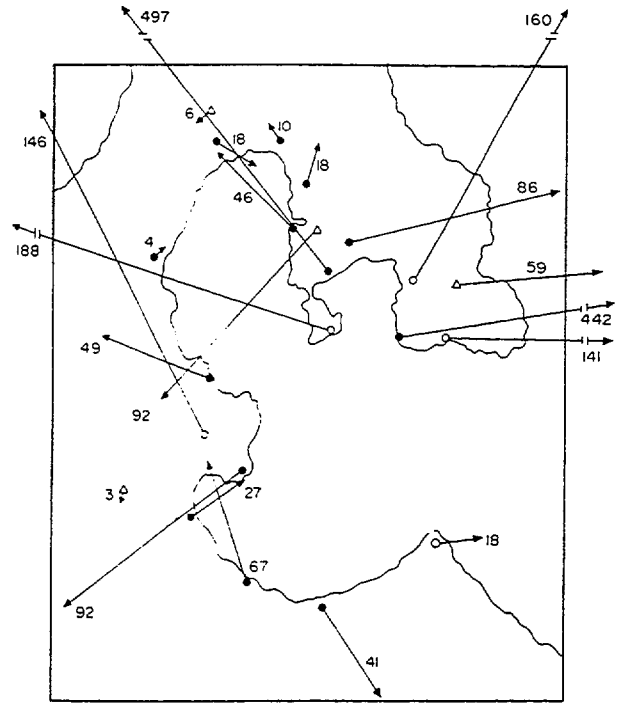


*Fig. 22. Tilt vectors (μrad) for the period October 1983 to July 1985. Open triangles denote water-tube tiltmeters, open circles denote dry tilt arrays installed 1980-81 and solid circles denote dry tilt arrays installed September 1983.*

Other significant results from the tilt monitoring program were the very low rates of tilt in the northern part of the caldera, in accord with the very small elevation changes there, and the negligibly small tilts from locations on the northern and western caldera walls. These results suggest that the deformation at Rabaul is due to localized intra-caldera sources.

*(iii) Horizontal deformation*

Horizontal deformation monitoring, using electronic distance measurements (EDM), was introduced at Rabaul Caldera during the Crisis Period. The station network consists of two base stations, RVO and MUKA (Fig. 23), on the caldera rim from which measurements are made to reflectors located within the caldera and also to a number of stations outside the caldera. The

pattern of horizontal deformation observed at Rabaul during the Crisis Period was divided into two time intervals which exclude the crisis of 3 March 1984 when the MUKA base station may have shifted.

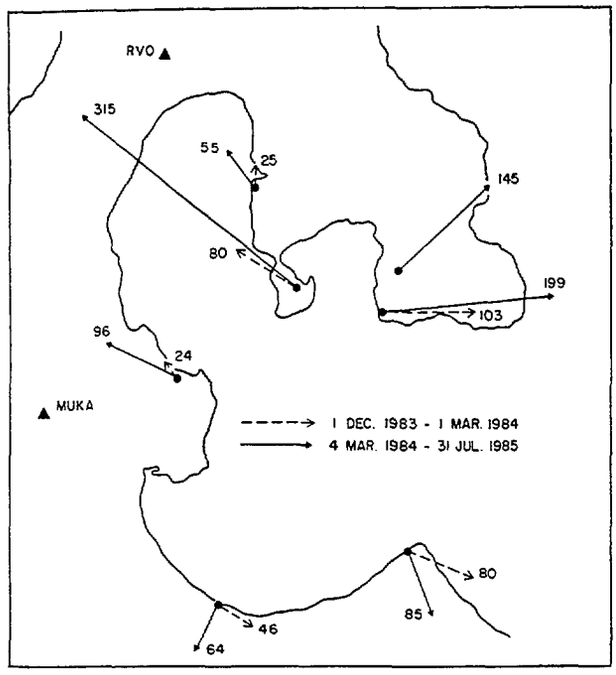


*Fig. 23. Horizontal distance changes (mm) for two periods between 1 December 1983 and 31 July 1985. Solid triangles mark the EDM base stations.*

A reasonably consistent pattern of horizontal deformation was observed for the northern half of the caldera, reflecting radially symmetric expansion centred at the mouth of Greet Harbour where the greatest individual station displacement was almost 400 mm (Fig. 23). The peak rates of expansion were about 25 microstrain per month across the mouth of Greet Harbour. EDM changes in the southern half of the caldera between December 1983 and March 1984 are reminiscent of the tilt changes in the same area, which suggest inflation about a source in the southwestern part of the caldera. For the period March 1984 to July 1985 the vectors for all of the stations in the caldera appear to radiate from a position near the mouth of Greet Harbour. Although this indicates the effect of a single deformation source, the vectors in the southern part of the caldera are larger than expected, and this combined with a slight rotation of the vector for a station near Vulcan, may imply continuing inflation, albeit weak, from a shallow source in the southwestern part of the caldera, and/or deformation from the inferred large magma reservoir which underlies the caldera (Mori et al., 1989).

Gravity

A program of gravity observations on a small network at Rabaul started in 1973 to check for possible temporal gravity changes. Levelling measurements on the gravity benchmarks commenced at the same time. Over the following two years the results indicated uplift of the ground and reduction in gravity values in the central part of the caldera. These results encouraged expansion of the network and inclusion of gravity monitoring in the long-term volcano surveillance program at Rabaul (McKee et al., 1989).

The distribution of the gravity changes (Fig. 24) on the expanded network was similar to that of elevation changes. Between September 1973 and the end of the Crisis Period (July 1985), the largest gravity change was about -410 $\mu$Gal measured at a station at the southern tip of Matupit Island. The same station was uplifted about 1.8 m over the same time interval (Fig. 25).

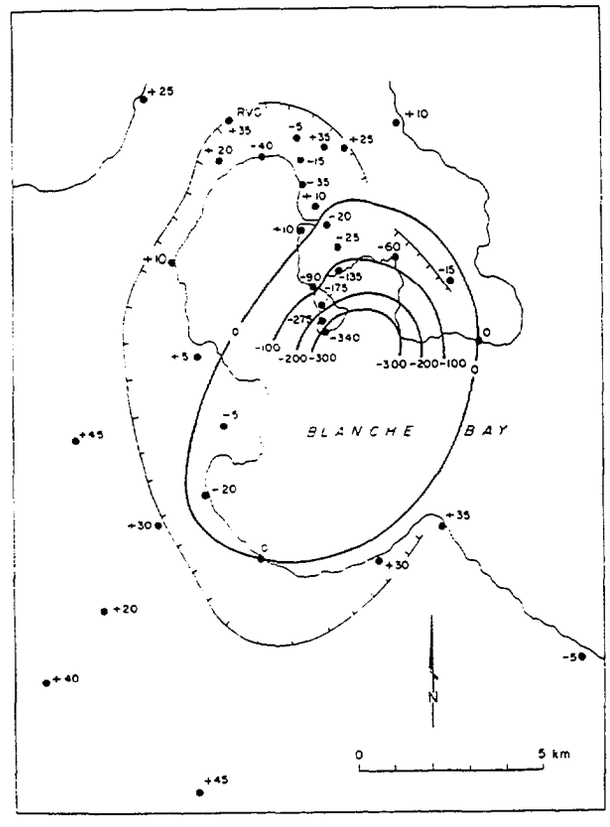


*Fig. 24. Net gravity changes (μgal) for the period January 1976 to July 1985.*

The relationship between gravity and elevation changes ($\Delta g/\Delta h$) in the period 1973-85 was -216 ± 4 $\mu$Gal/m where the uncertainty is 1 standard deviation. This value of $\Delta g/\Delta h$ is indicative of sub-surface mass changes, presumed to be due to input of magma.

The strong negative correlation between the gravity and uplift data extended throughout the uplifted area (Fig. 26). The sharp decay in both quantities with distance from Matupit Island indicates a shallow source for these effects, which can be adequately modelled by a "point" source (Mogi, 1958). Analysis of the levelling data indicated that the depth of the source remained steady at abut 1.8 km. Figure 26 shows the theoretical values of uplift and gravity change for a point source at a depth of 1.8 km located near the mouth of Greet Harbour.

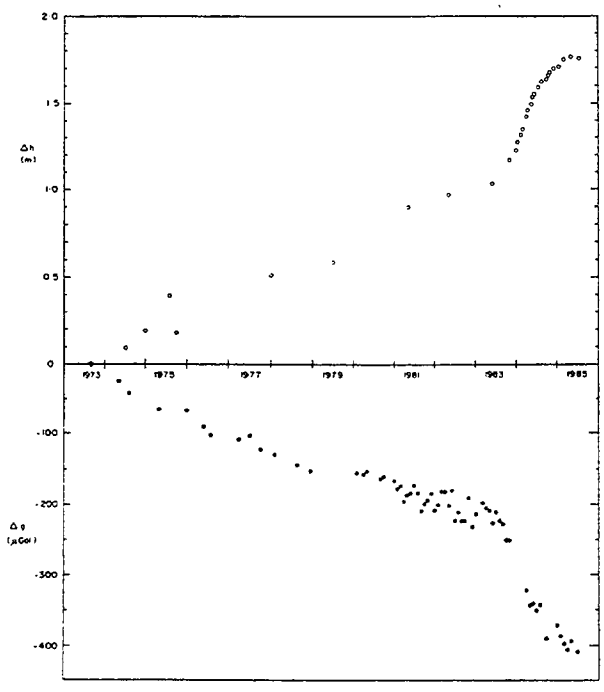

*Fig. 25. Gravity and elevation change at the southern tip of Matupit Island in the period September 1973 to July 1985.*

Using Gauss's Theorem, the excess mass which accumulated at the Greet Harbour source in the period 1973-85 was estimated from the gravity data to be 1.0 x $10^8$t. Assuming this is magma having a density of 2.5 t/m$^3$, which is appropriate for hydrous, intermediate composition magma at a depth of several kilometres (Kushiro, 1978), the intruded magma would have a volume of 40 x $10^6$ m$^3$.

The consistency of the depth of source estimates may suggest that the source is a well-established feature that can accommodate the input of small to moderate volumes of magma without causing an eruption. Past activity at this source could explain the previous reports of ground deformation in the Sulphur Creek-Matupit Island area between eruptions. Perhaps more

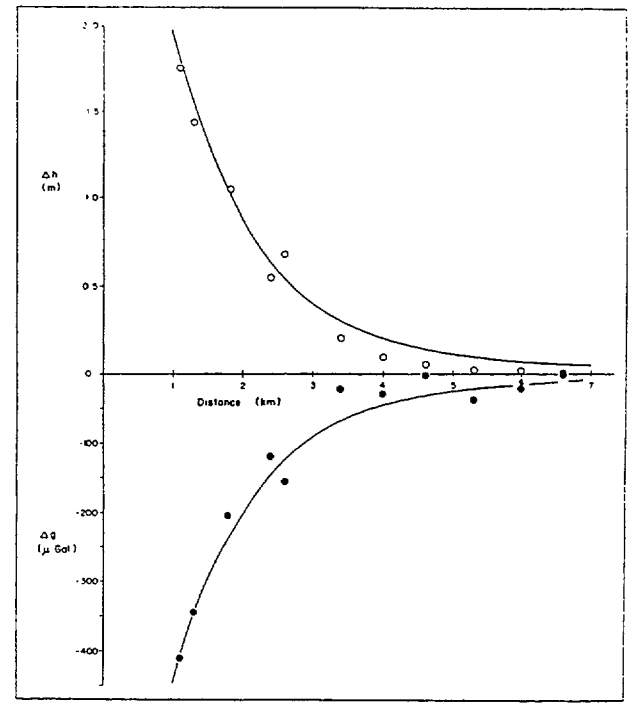


*Fig. 26. Gravity and elevation changes vs radial distance from the assumed position of the source of these changes. The curved lines are the theoretical effects of a point source at a depth of 1.8 m.*

importantly, pre-historical intrusion(s) in this area may be indicated by geological features exposed in a cliff at the southern end of Matupit Island, and detected offshore by marine seismic reflection surveys. Layered tephra deposits in the cliff have been arched upwards and the axial part of the resultant anticline has subsided along a set of stepped normal faults (Nairn et al., 1989). Draping the faulted anticline is a thin layer of re-worked pumiceous sands and gravels, which contain coral and shell fragments. Up-bowing and north-south oriented faulting is also evident offshore, to the south of Matupit Island (Greene et al., 1986). This evidence of uplift and deformation is consistent with pre-historical caldera resurgence due to upward migration and accumulation of magma within the caldera.

## ACKNOWLEDGEMENTS

For assistance and support during the preparation of this excursion guide, we are sincerely grateful to our colleagues at RVO, namely Pavora Marupi, Nick Lauer, Rod Stewart, David Lolok and Elmah Rukie.

REFERENCES

Anderson E.M., 1936: The dynamics of the formation of cone sheets, ring-dykes and cauldron subsidences. **Proceedings of the Royal Society of Edinburgh 56**: 128-163.

Bloom A.L., Broecker W.S., Chappell J.M.A., Matthews R.K., Mesolella K.J., 1974: Quaternary sea level fluctuations on a tectonic coast: new $^{230}Th/^{234}U$ dates from the Huon Peninsula, New Guinea. **Quaternary Research 4:** 185-205.

Brown G., 1878: Journal of the Rev. G. Brown, 1860-1902, (11 volumes). **Mitchell Library**, Sydney Australia.

Chappell J., Shackleton N.J., 1986: Oxygen isotopes and sea level. **Nature 324:** 137-140.

Crick I.H., 1975: Investigation into a change in topography at Rabaul Golf Course. **Geological Survey of Papua New Guinea Report 75/6**: 5p (unpublished).

Ewart A., 1982: The mineralogy and petrology of Tertiary-Recent orogenic volcanic rocks: with special reference to the andesite-basaltic compositional range. In: R.S. Thorpe (ed.) **Andesites: Orogenic Andesites and Related Rocks**. John Wiley & Sons, Chichester: 25-95.

Fisher N.H., 1939: Geology and vulcanology of Blanche Bay and the surrounding area, New Britain. **Territory of New Guinea, Geological Bulletin 1**: 68p.

Fisher N.H., 1976: 1941-42 eruption of Tavurvur volcano, Rabaul, Papua New Guinea. In: R.W. Johnson (ed.). **Volcanism in Australasia**. Elsevier Scientific Publishing Company, Amsterdam: 201-210.

Gill J.B., 1981: **Orogenic Andesites and Plate Tectonics**. Springer-Verlag, Berlin.

Greene H.G., Tiffin D.L., McKee C.O., 1986: Structural deformation and sedimentation in an active caldera, Rabaul, Papua New Guinea. **Journal of Volcanology and Geothermal Research 30**: 327-356.

Heming R.F., 1974: Geology and petrology of Rabaul Caldera, Papua New Guinea. **Bulletin of the Geological Society of America 85**: 1253-1264.

Heming R.F., Carmichael I.S.E., 1973: High-temperature pumice flows from the Rabaul Caldera, Papua New Guinea. **Contributions to Mineralogy and Petrology 38**: 1-20.

Kushiro I., 1978: Density and viscosity of hydrous calc-alkalic andesite magma at high pressures. **Carnegie Institute of Washington Year Book 77**: 675-677.

Lafehr, T.R., 1965: The estimation of the total amount of anomalous mass by Gauss's theorem. **Journal of Geophysical Research 70**: 1911-1919.

Lindley D., 1988: Early Cainozoic stratigraphy and structure of the Gazelle Peninsula, East New Britain: An example of extensional tectonics in the New Britain arc-trench complex. **Australian Journal of Earth Sciences 35**: 231-244.

McKee C.O., Lowenstein P.L., de Saint Ours P., Talai B., Itikarai I., Mori J.J., 1984: Seismic and ground deformation crises at Rabaul Caldera: prelude to an eruption?: **Bulletin Volcanologique 47**: 397-411.

McKee C.O., Johnson R.W., Lowenstein P.L., Riley S.J., Blong R.J., de Saint Ours P., Talai B., 1985: Rabaul Caldera, Papua New Guinea: volcanic hazards, surveillance, and eruption contingency planning. **Journal of Volcanology and Geothermal Research 23**: 195-237.

McKee C.O., Mori J., Talai B., 1989: Microgravity changes and ground deformation at Rabaul Caldera, 1973-1985. In: J.H. Latter (ed.) **IAVCEI Proceedings in Volcanology, Vol. 1 Volcanic Hazards.** Springer-Verlag, Berlin: 399-428.

Mogi K., 1958: Relations between the eruptions of various volcanoes and the deformations of the ground surface around them. **Bulletin of the Earthquake Research Institute 36**: 94-134.

Mori J., McKee C., 1987: Outward-dipping ring-fault structure at Rabaul Caldera as shown by earthquake locations. **Science 235**: 193-195.

Mori, J., McKee C.O., de Saint Ours P., Itikarai I., 1987: Sea level measurements for inferring ground deformations in Rabaul Caldera. **Geo-Marine Letters 6**: 241-246.

Mori J., McKee C.O., Itikarai I., Lowenstein P.L., de Saint Ours P., Talai B., 1989: Earthquakes of the Rabaul seismo-deformational crisis September 1983 to July 1985: Seismicity on a caldera ring fault. In: J.H. Latter (ed.) **IAVCEI Proceedings in Volcanology, Vol.1 Volcanic Hazards**. Springer-Verlag, Berlin: 429-462.

Nairn I.A., Wood C.P., Talai B., McKee C.O., 1989: Rabaul Caldera, Papua New Guinea - 1:25 000 reconnaissance geological map and eruption history. **New Zealand Geological Survey**: 76p.

Newhall C.G., Dzurisin D., 1988: Historical unrest at large calderas of the world. **U.S. Geological Survey Bulletin 1855**: 1108p.

Rubin A.M., Pollard D.D., 1988: Dike-induced faulting in rift zones of Iceland and Afar. **Geology 16**: 413-417.

Sapper K., 1910: Beitraege zur Kenntnis Neupommerns und des Kaiser-Whilhelmsland, **Petermanns Mitteilungen 56**: 189-193 and 255-256 (in German).

Schleinitz G.E.G., 1889: Die Forschungreise S.M.S. "Gazelle" in den Jahren 1874 bis 1876 unter Kommando des Kapitan zur see Freiherrn von Schleinitz Herausgegeben von dem Hydrographischen Amtdes Reichs-Marine-Amts. I. Thiel. der Reisebericht. Mittler & Sohn, Berlin (in German).

Scott B.J., 1982: Tiltmeter recordings at Rabaul Caldera Papua New Guinea: 1963-1979. **Geological Survey of Papua New Guinea Report 80/13**: 12p (unpublished).

Sheridan M.F., Wohletz K.H., 1983: Hydrovolcanism; basic considerations and review. **Journal of Volcanology and Geothermal Research 17**: 1-29.

Simpson C.H., 1873: Hydrographical extract from a six months cruise among the South Sea Islands. **Report to the Admiralty, 11 December 1872, Great Britain, Parliamentary Accounts and Papers, Session 6 February - 5 August 1873, Colonies and British Possessions**: 1-50.

Taylor B., 1991: Rabaul Caldera, Papua New Guinea, SeaMARC II sidescan sonar imagery, aerial photography, bathymetry, and topography, 1:25,000, **Pacific Seafloor Atlas**, Hawaii Institute of Geophysics, Honolulu, Sheet no. 8.

Walker G.P.L., 1983: Ignimbrite types and ignimbrite problems. **Journal of Volcanology and Geothermal Research 17**: 65-88.

Walker G.P.L., Heming R.F., Wilson C.J.N., 1980: Low aspect ratio ignimbrites. **Nature 283**: 286-287.

Walker G.P.L., Heming R.F., Sprod T.J., Walker H.R., 1981: Latest major eruptions of Rabaul Volcano. In R.W. Johnson (ed.) Cooke-Ravian Volume of Volcanological Papers. **Geological Survey of Papua New Guinea Memoir 10**: 181-193.

Wohletz K.J., 1983: Mechanisms of hydrovolcanic pyroclastic formation: size, scanning electron microscopy, and experimental results. **Journal of Volcanology and Geothermal Research 17**: 31-63.

## EXCURSION ROUTE

## STOP DESCRIPTIONS

Day 1 RVO, caldera unrest, historical volcanism

*Stop 1 — RVO*

RVO is located on the northern rim of Rabaul Caldera at an elevation of 185 m a.s.l. (Fig. 27). The observatory was established in 1940 as a consequence of the damaging eruptions in 1937 to provide warnings of future activity. It was destroyed by bombing during World War II. Reconstruction started in 1950 and major extensions and additions were made in 1969. The present RVO is the centre for volcanological investigations throughout Papua New Guinea, although Rabaul remains the focus of the RVO monitoring program.

The only eruption that has taken place at Rabaul since the establishment of RVO was the 1941-43 activity at Tavurvur. Over 6 months of precursory activity at Tavurvur was monitored prior to the outbreak there of mild explosive activity in June 1941.

An intriguing episode of increased seismicity and ground deformation was tracked through the 1970's and early 1980's. The peak of this phase of caldera unrest was reached in 1984 and passed without leading to an eruption.

The visit to RVO will provide an opportunity to examine the volcano monitoring program and its results.

*Stop 2 — Matupit Island, uplifted pumice sediments*

Exposures at Matupit Island provide evidence of recent uplift and longer-term resurgence within Rabaul Caldera. This island is composed primarily of the Matupit Pumice Sediments which are water-sorted, sea-rafted dacitic pumice lapilli and ash beds. These pumiceous sediments are stratified into poorly-sorted ash-dominated and better-sorted lapilli-dominated parallel bedded layers. The ash-dominated beds show low-angle cross bedding. The coarse layers are commonly reverse-graded and sometimes slightly imbricated. Pumice lapilli usually show some rounding but larger clasts are more angular. Light and dark grey pumices are present, together with some banded pumice. Rare dense lithic clasts are present but have no underlying impact sags.

The source of the Matupit Pumice Sediments is not known. The exposures at Matupit Island are the coarsest but the lack of large pumice clasts and paucity of lithic clasts and impact sags suggests that the eruptive source is elsewhere. The sediments probably resulted from a submarine eruption within the caldera, with deposition from water logging of pumice rafts. They may have been erupted from the vent which produced the Dawapia Rocks.

The undisturbed pumice sediments are overlain by reworked pumiceous sands and gravels containing coral and shell fragments, and by younger subaerial tephras. Shell and coral samples from the reworked upper pumice sediments at Matupit Island have given $^{14}C$ dates which average at about 750 yrs BP. The base of the Matupit Pumice Sediments is not exposed, the greatest thickness above sea level being about 17 m.

In the early 1970's the southern shore of Matupit Island was at the base of the cliffs exposing the Matupit Pumice Sediments. Uplift of about 2 m has taken place over the past two decades. The newly emerged foreshore has been planted with coconuts.

Longer-term uplift or resurgence has resulted in gentle arching of the layered pumice sediments. This broad anticline is cut by a keystone graben near its apex. These structures are probably related to a series of north-trending normal faults detected offshore to the south (Greene et al., 1986). A simple calculation based on the greatest thickness of emerged Matupit Pumice Sediments and the age of the reworked layers at the top of the sediments gives an average resurgence rate of about 2 cm/yr at this locality.

*Stop 3 — Tavurvur 1937 tephra*

The Tavurvur 1937-43 Pyroclastics comprise the altered cone material and minor fresh andesite/dacite ash and blocks erupted from Tavurvur Cone and small explosion craters on the cone's flanks during the 1937-43 eruptive period. The tephra of the (1-day) 1937 eruption of Tavurvur was dispersed in a narrow fan trending northwest, and as much as about 7 cm of ash was deposited on Rabaul township. The 1941-43 ejecta is now recognisable only in the immediate vicinity of Tavurvur Cone.

At this locality, about 1.7 km northwest of the summit of Tavurvur, the 1937 ash is about 1 m thick. This phreatomagmatic ash is dark grey, fine-grained and shower-bedded. Interspersed thin layers and lenses of pale fine-grained pumiceous ash originated at Vulcan which was simultaneously erupting. Weak cross-bedding in the dark Tavurvur ash is evident in some exposures.

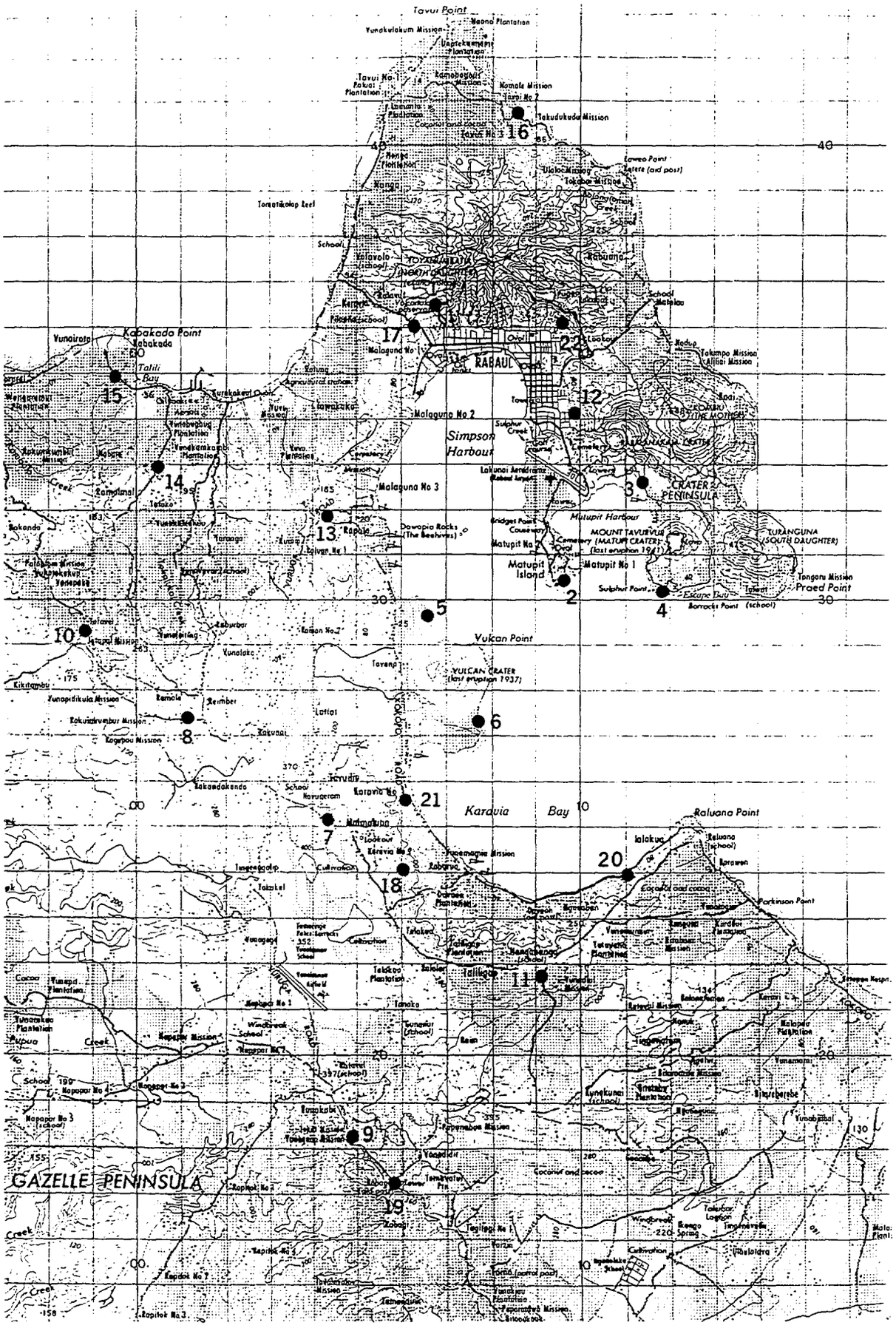


*Fig. 27. Rabaul area and locations of major excursion stops. Grid spacing is 1 km.*

Tephra deposits from several earlier eruptions of Tavurvur are also exposed at this locality. In turn these deposits overlie pneumatolytically altered tephra though to have originated at Rabalanakaia Crater about 1 km to the northwest. All of these tephra deposits overlie a lava flow from Rabalanakaia which entered the sea at the head of Greet Harbour.

*Stop 4 — Tavurvur 1878 tephra*

Andesitic (?) and altered lithic tephra was erupted from Tavurvur in 1878 (simultaneously with activity at Vulcan Island) and was mostly dispersed southeast of the vent. The duration of the eruption was at least two weeks. A small cratered cone was formed at the southern part of Tavurvur's summit by this activity.

The Tavurvur 1878 tephra consists of finely bedded fine and coarse ash layers totalling about 2 m at this locality. Phreatic conditions are indicated for part of the eruption. The lower part of this exposure consists of very hard, coherent, finely laminated fine ash. About 1.2 m above the base there is a gradual change to a softer, friable ash with numerous vesicles. Accretionary lapilli are abundant. The scoriaceous andesitic (?) coarse ash is of magmatic origin.

About 6 m of uplift took place in this area at the time of the 1878 eruption. The nature of the 1878 tephra suggests that the uplift took place before the eruption started.

*Stop 5 — Vulcan 1937 tephra*

The eruption that formed Vulcan Cone took place in the period 29 May - 1 June 1937. The speed at which the eruption developed, and the rate at which tephra was expelled from the vent, were so great that people within 2-3 km of the volcano had little chance of escape. C.A. Wood (1980) reported that Vulcan Cone grew the fastest of 12 historically produced "cinder" cones studied by him in a literature search. Multiple vents were active in the formation of the cone and the adjacent pyroclastic surge fans. Interbedded Plinian ash and lapilli beds were dispersed in a broad bi-lobed fan to the west and north. The tephra of this eruption is dominated by high-K andesitic/dacitic pumice.

Pyroclastic surge beds about 1 km north of the cone show low-angle cross-bedding. The coastal cliffs at the northern foot of the cone expose up to 20 m of poorly sorted pyroclastic surge and fall beds containing abundant fine ash-coated pumice clasts and dark grey to black vesicular bombs and lithic blocks in a grey ash matrix. Some pumice shows faint banding. The Plinian beds mantling the country west of the cone contain well-sorted and shower-bedded fall units, and are interbedded with surge deposits in proximal sections on the Kokopo Road immediately west of Vulcan Cone.

*Stop 6 — Vulcan 1878 tephra*

The eruption that produced Vulcan Island in 1878 was of short duration (a few days) and was largely submarine. There was no widespread airfall tephra but huge pumice rafts were formed. Vulcan Island was of low relief attaining a maximum height of only 18 m a.s.l. The main vent appears to have been at the southern end of the island. The Vulcan 1878 tephra is chemically very similar to the material of the 1937 eruption, i.e. high-K andesite/dacite. Some Vulcan 1878 pumice is streaky.

Sea cliffs about 1 km southeast of Vulcan Cone expose about 6+ m of Vulcan 1878 tephra. The lower 2+ m is chaotically bedded and consists of broken large dark pumice blocks and dense angular lithics almost clast-supported in a minor ash matrix. Deposition was from submarine surges and sea-rafting.

The 4+ m upper section displays low-angle cross-bedding in ashy material, lacking large pumice clasts but containing common dense lithics as much as 150 mm in size. These beds appear to have originated from wet but subaerial base surges produced when the vent had risen above sea level.

About 100-150 m south of the Vulcan tide gauge a layer of coarse pale brown Vulcan 1878 pumice clasts is seen to gradually lens out to the north. Beach deposits rich in shells and coral are present at both upper and lower surfaces of the pumice layer. The lower contact is with a pre-1878 shoal consisting of dark-medium grey-brown dense pumice lapilli, glassy clasts and coarse ash, possibly the products of an earlier eruption in this area.

## Day 2 Rabaul Pyroclastics

The Rabaul Pyroclastics are dacitic, mostly non-welded pyroclastic flows and underlying Plinian and fine-medium ashfall beds which were erupted at c. 1400 yrs BP ($^{14}C$ dates) in the latest caldera-forming eruption at Rabaul. These units were informally termed the "Rabaul plinian pumice-fall" deposit, and the "Rabaul ignimbrite" by Walker et al. (1981) and are defined as members of the Rabaul Pyroclastics Formation (Nairn et al., 1989). The extremely violent high energy pyroclastic flows covered the entire Rabaul area, travelled over the sea to Watom Island, and overlie even the highest peaks of Tovanumbatir and Kombiu. A full description of the Rabaul Pyroclastics and their eruption mechanisms is given by Walker et al. (1981).

*Stop 7 — Plinian pumice - fine and medium ashes — Malmaluan*

The Rabaul Plinian pumice-fall deposit consists mostly of coarse pumice, and is widely dispersed west of the caldera where it reaches a maximum observed thickness of about 130 cm. In general, the pumice is pale grey although some coarse clasts are pink to brown due to oxidation. Lithic clasts constitute about 5 weight percent of the deposit - black obsidian is the most common lithic material. Two or three prominent bimodal layers of fine ash mingled with pumice lapilli, a few cm thick, are interbedded with the coarse pumice over most of the dispersal area. The fact that the coarser pumice in the bimodal layers is identical to that in the underlying and overlying Plinian deposit may indicate that the bimodal beds do not mark interruptions in the Plinian phase. The fine ash may have been flushed out of the ash cloud by rain. Isopach and isopleth maps of the Rabaul Plinian pumice-fall deposit (Fig. 28) suggest that the source vent is now submerged beneath the sea in the central part of the caldera. The present locality near the southwestern rim of the caldera is about 6 km from the inferred position of the vent.

The broad dispersal of the Plinian pumice is indicative of a high eruption column. There is a very slight overall reverse grading. The pumice is moderately well-sorted having sorting coefficient values in the range 1.3-2.0. However some of the larger pumice clasts were broken during accumulation and subsequent compaction of the deposit.

The volume of the deposit on land within the area shown in Figure 28 is 0.37 $km^3$. Calculations indicate that the true volume may be about 1.66 $km^3$.

Apart from the fine ash layers interbedded with the coarse pumice, there are fine-medium air-fall ashes both below and above it. The lower deposit is fine-medium grained ash dispersed over a narrow fan west and northwest of the caldera. The general orientation of this dispersal is similar to that of the Vulcan 1937 eruption (Fig. 17). The narrowness of the dispersal fan and the fine grainsize indicate that this initial phase of activity was relatively mild. The maximum observed thickness of this deposit is 16 cm.

Overlying the Plinian deposit is a poorly stratified succession of mostly fine ashes. The total thickness of these deposits in most exposures is 35-40 cm. They are much more laterally extensive than the Plinian pumice but probably have a similar volume. One ash bed near the top of this succession has abundant vesicles of irregular shape formed by trapping of air bubbles, and small accretionary lapilli. These ashes are probably of phreato-Plinian type as indicated by fine grainsize and wide dispersal.

At the top of the airfall sequence is a 5-10 cm layer containing coarse pumice and lithic clasts, together with fine material, giving it a strongly bimodal grainsize distribution. The pumice and lithic clast sizes are larger in this bed than in the Plinian deposit indicating more powerful activity immediately preceding the ignimbrite-generating phase of the eruption.

*Stop 8 — Ground layer —Rakunai*

A lithic and crystal rich lapilli or ash grade deposit is found at the base of the ignimbrite and locally between flow units. This is interpreted to be the "ground layer". The thickness of this deposit ranges between about 2 m near the caldera to a few cm at distal locations, although the variation of thickness with distance from source is irregular, a feature attributed to the shearing and erosion of this "head" deposit by the body of the over-riding pyroclastic flow. The maximum lithic clast size is about 1 m near the caldera, decreasing to about 1 cm at a distance of 25 km (Fig. 29D).

At this location, about 10 km from inferred position of the source of the Rabaul Ignimbrite, the ground layer is about 1 m thick. The deposit is virtually structureless.

*Stop 9 — Ignimbrite veneer deposit — Vunadidir*

The ignimbrite veneer deposit (IVD) comprises between half and three-quarters of the total volume of the Rabaul Ignimbrite. The IVD is a blanket-type deposit containing lenses of well-sorted and well-rounded pumice clasts. The lenses are best developed on ridge tops and other topographic high features. In places, a gradation into valley-fill ignimbrite can be observed. The distribution of IVD is shown in Figure 29A.

The maximum pumice size decreases from several tens of cm in or near the caldera to 2 cm or less at a distance of 25 km. The size of lithic clasts decreases from 10 cm or more in or near the caldera to about 1 cm at distances of 15-20 km (Fig. 29C).

At the present locality, about 12 km from source, the IVD is about 10 m thick.

*Stop 10 — Valley-fill ignimbrite —Totovel*

The valley-fill or normal ignimbrite is coarser than the IVD on the interfluves. Pale highly expanded pumice clasts, up to several tens of cm in size, are present at proximal locations although the median diameter of pumice clasts ranges between about 4 mm and ¼ mm at distances of less than 10 km from source. At greater distances the median diameter of pumices ranges

between about ¼ mm and 1/32 mm. Other large juvenile fragments are black vesicular obsidian.

The valley-fill ignimbrite is structureless. Its thickness may be as much as 30 m where it has ponded in deep pre-existing valleys. Even at its thickest, no welding is evident. At the present locality the ignimbrite is at least 10 m thick (base not seen).

*Stop 11 — Fines-depleted ignimbrite —Nangananga*

Fines-depleted ignimbrite (FDI) is an important variant of normal ignimbrite at Rabaul. FDI can be extremely coarse and has an abnormally low content of fine-grained material. Patches or lenses of FDI are reasonably common and in some places the entire flow deposit is FDI.

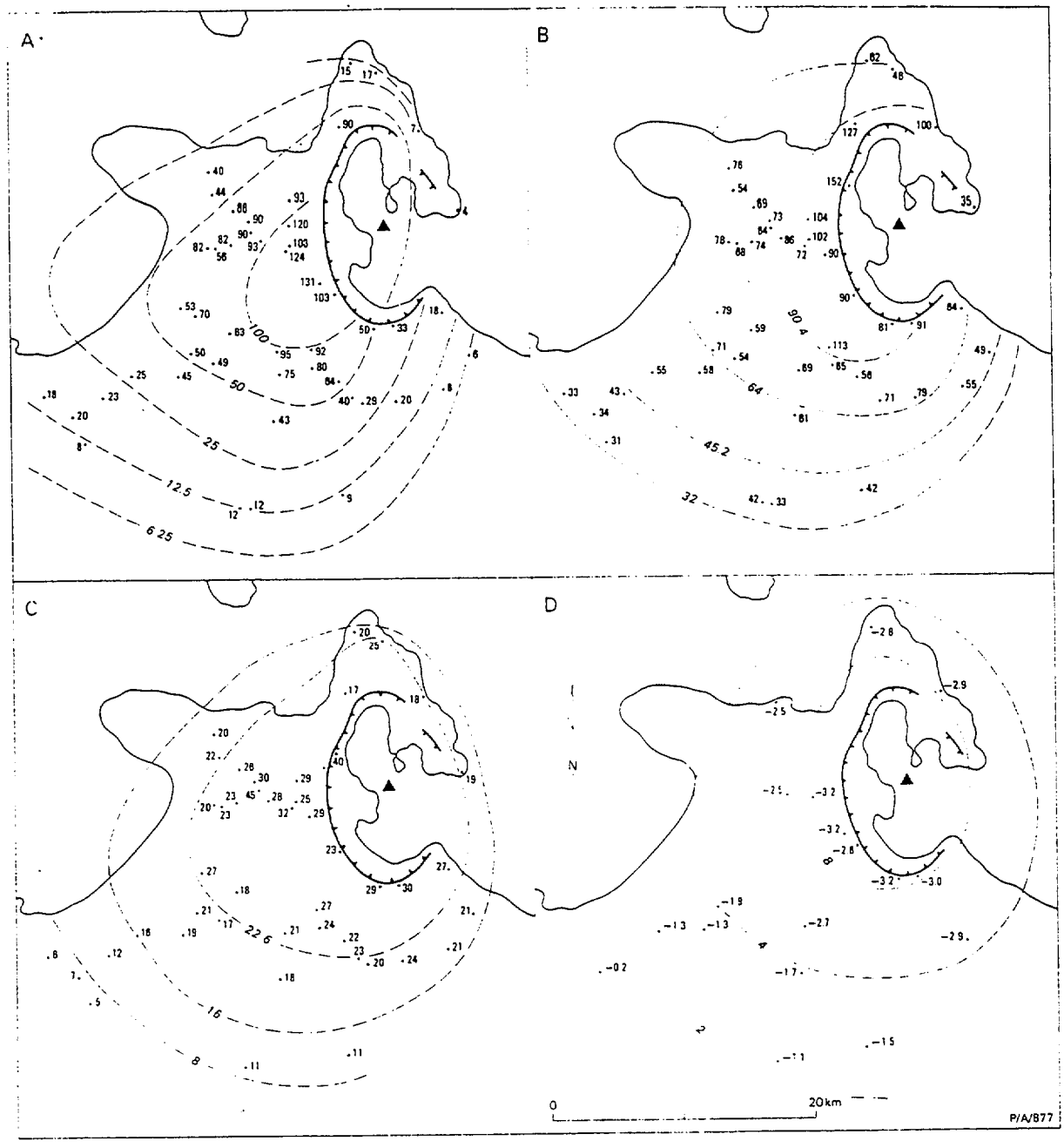


*Fig. 28. Dispersal maps for the 1400 BP Rabaul Plinian pumice-fall deposit (after Walker et al., 1981). Triangles represent inferred vent position. A: deposit thickness (cm). B: average maximum diameter (mm) of the three largest pumice clasts. C: average maximum diameter (mm) of the three largest lithic clasts. D: median diameter (values in ϕ units, isopleths in mm) given by sieved samples from the coarsest part of the deposit.*

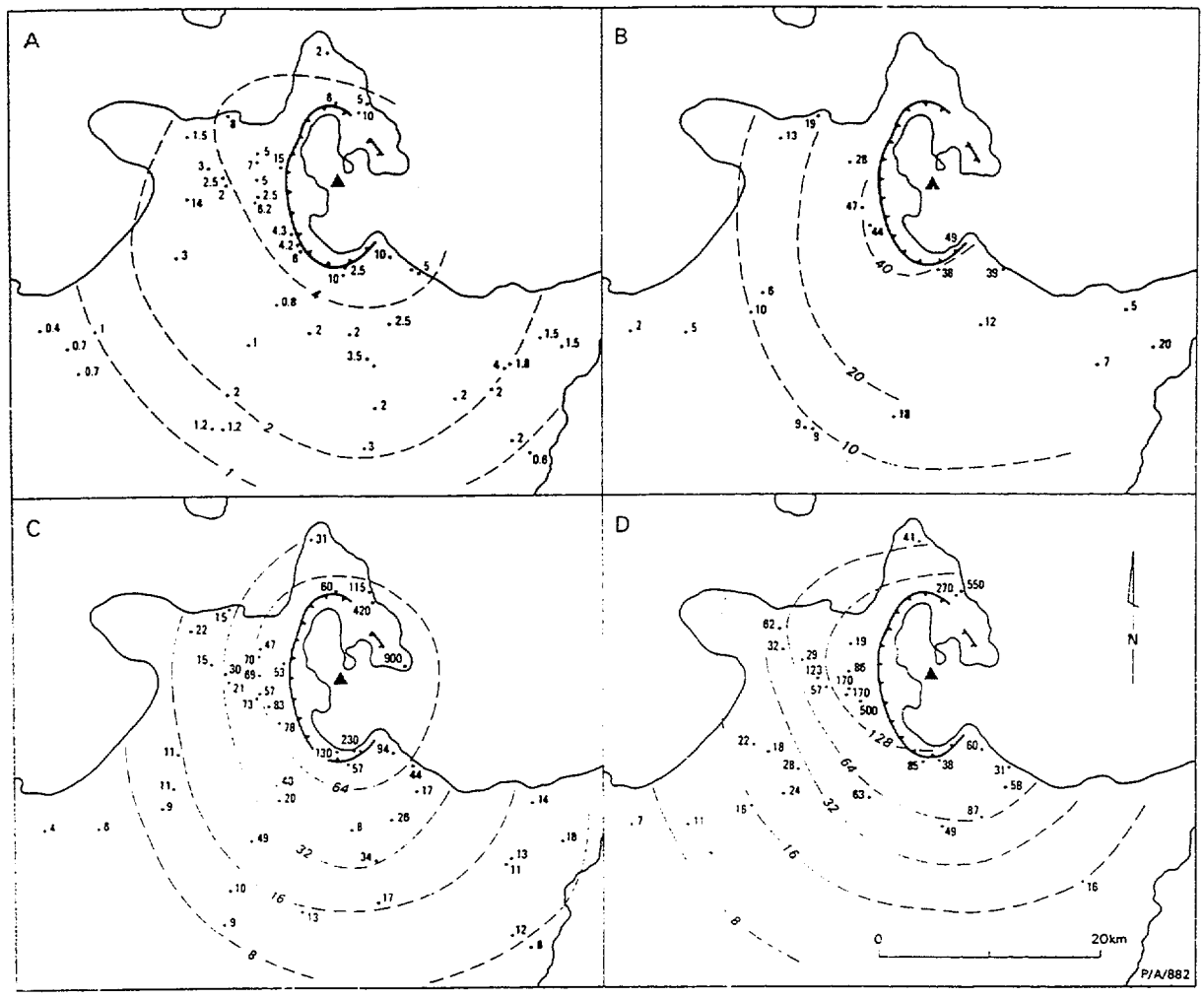


*Fig. 29. Dispersal maps for the 1400 BP Rabaul Ignimbrite (after Walker et al., 1981). A: approximate thickness (m) of the blanket-type (IVD) ignimbrite. B: weight percentage of material 1 mm or coarser in sieved samples of the ignimbrite. C: average maximum diameter (mm) of the three largest lithic clasts in the blanket-type ignimbrite. D: average maximum diameter (mm) of the three largest lithic clasts in the ground layer.*

Compared with normal ignimbrite, FDI is coarser and somewhat better sorted. The contrasts in grain-size characteristics between FDI and normal ignimbrite can be seen in the histograms and cumulative curves of Figures 30 and 31. As with normal ignimbrite, FDI contains large juvenile clasts of black vesicular obsidian at some localities.

The FDI contains larger lithic fragments than normal ignimbrite at the same locality. The lithic clasts are scattered throughout the FDI which may indicate a high degree of turbulence in the flow. Strong turbulence may have been induced by flow over rugged terrain. It should be noted that on the western and southern flanks of Rabaul Volcano, where the drainage is parallel to the caldera outline, flow would have been across valleys rather than along them, a situation likely to promote strong turbulence.

Where two flow deposits are present, FDI is invariably the lower one, overlain by normal ignimbrite. This relationship is shown at the present locality near the southern rim of the caldera. The FDI deposit here is about 5 m thick overlain by a similar thickness of normal ignimbrite. The boundary between the two ignimbrite types is a near-planar surface sloping 4° southwards. The FDI contains carbonised logs oriented approximately radially to the vent.

Day 3 Earlier Eruptives I

*Stop 12 — Raluan Pyroclastics, Talili Pyroclastics — Adelaide Street*

The Raluan Pyroclastics comprise a rhyolitic ignimbrite member and a coeval underlying basaltic scoria fall member. The contact between the two members is

unconformable in some exposures (in places the ignimbrite has totally eroded the scoria), but no weathering or erosional break between the two deposits is evident in conformable contacts. Walker et al. (1981) described the Raluan Ignimbrite as the "Penultimate Ignimbrite", pre-dating the Rabaul Pyroclastics. Multiple smaller eruptions between these two major events produced the Talili Pyroclastics. Recent work indicates that the date of the Raluan eruption was c. 6800 yrs BP ($^{14}C$).

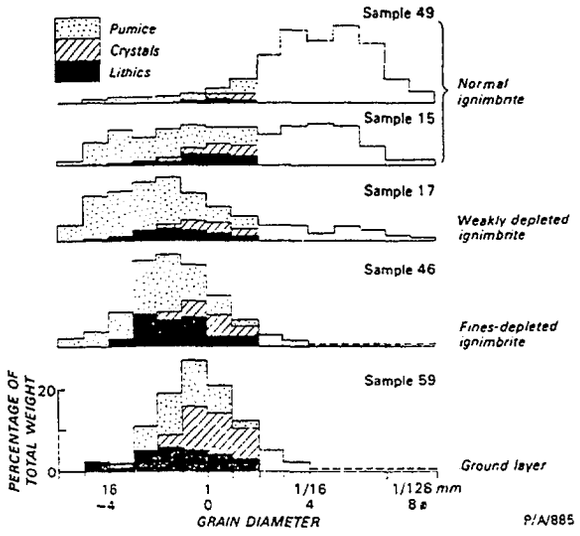


*Fig. 30. Grain-size histograms for typical samples of normal Rabaul ignimbrite, weakly depleted ignimbrite, fines-depleted ignimbrite, and ground layer. Only those classes ¼ mm and coarser are subdivided according to the proportions of components present (after Walker et al., 1981).*

The basaltic scoria member consists of loose shower-bedded black basaltic scoria overlying a well-developed palaeosol. The deposit is well sorted having sorting coefficient values of 0.95 to 1.25. A brown oxidised band is commonly found near the middle of the deposit. The maximum thickness recorded is 5.8 m of ash to block size scoria (including dense juvenile clasts) in a gully immediately east of Adelaide Street. At the present locality the scoria deposit is about 4 m thick. The source of the scoria appears to have been in the northeastern part of the Rabaul complex and distribution was to the west (Fig. 32). The moderately widespread dispersal suggests a sub-plinian mode of eruption.

The overlying ignimbrite is a white, non-welded rhyolitic pyroclastic flow deposit, containing large white fibrous pumice blocks at localities near the caldera. The thickness of the ignimbrite ranges from about 20 cm to several m. An associated (rhyolitic) plinian fall deposit is absent suggesting that no high eruption column preceded the ignimbrite eruption. The mineralogy and chemistry of the Raluan Ignimbrite are distinctive. It is almost unique at Rabaul in having as constituents quartz and hornblende. Chemical analyses of pumice clasts from the Raluan Ignimbrite have low $K_2O$, Rb, Sr, Zr and Ba contents.

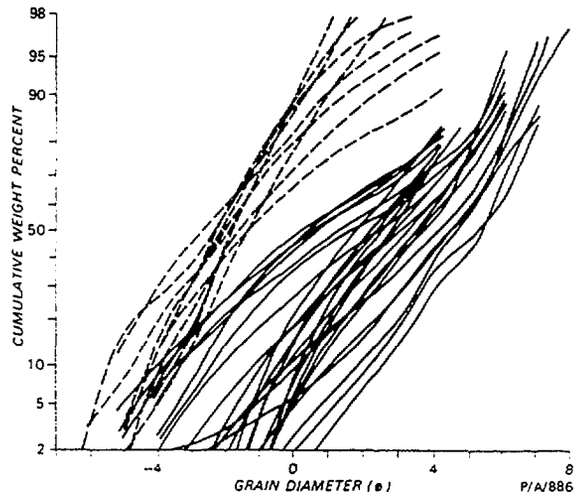


*Fig. 31. Cumulative weight percentage coarser than the indicated grain size for samples of normal Rabaul ignimbrite (solid lines) and for samples of weakly depleted and fines-depleted ignimbrite (dashed lines). (After Walker et al., 1981).*

Walker et al. (1981) presumed that the ignimbrite was erupted from the same vent as the scoria which they considered (from limited dispersal data) to be within Simpson Harbour, near Matupit Island. The work of Nairn et al. (1989) indicated that while the ignimbrite was probably erupted from a Simpson Harbour source, the vent for the scoria was probably several km northeastwards, at Palangiagia or Kombiu.

The maximum lithic and pumice clast sizes in the ignimbrite are similar, and range from about 7 cm near the caldera rim to 1 cm about 15 km farther out. The distribution and thickness of the ignimbrite are those of blanket-type ignimbrites (IVD). From limited data it is estimated that the volume of this ignimbrite is about half that of the succeeding (Rabaul) ignimbrite, i.e. about 5 $km^3$. The volume of the scoria may be an order of magnitude smaller.

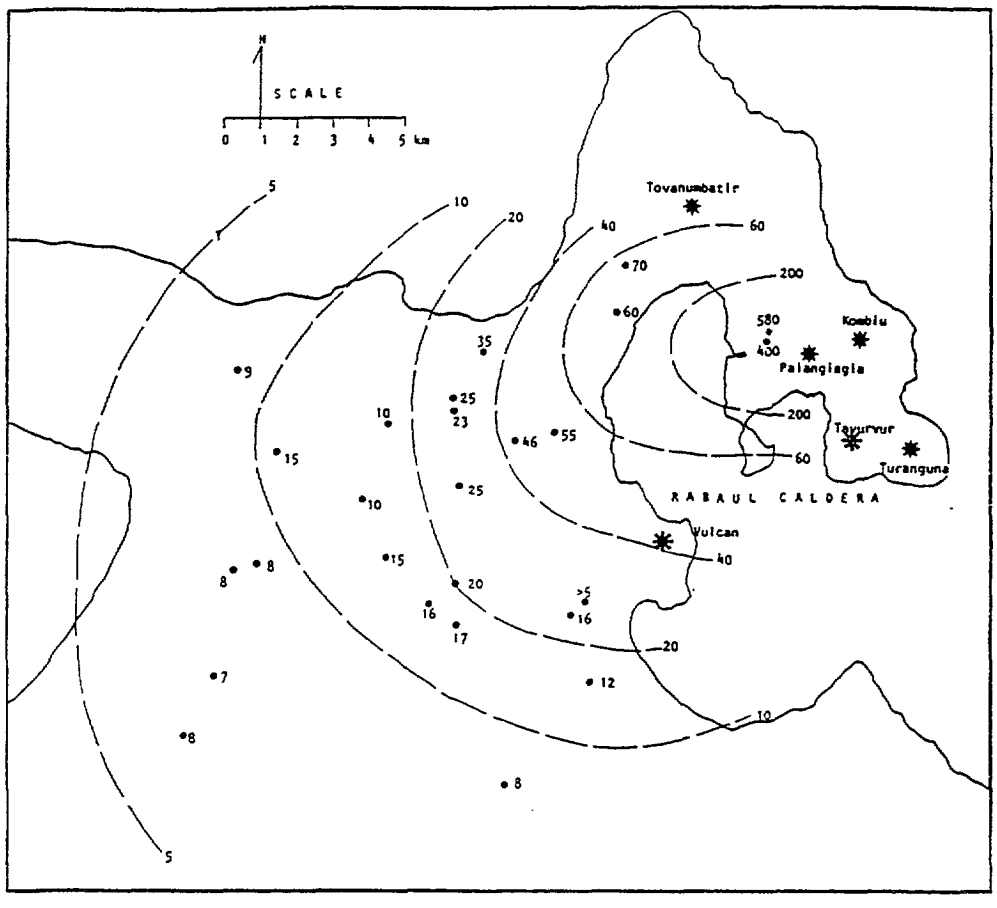


*Fig. 32. Distribution of the Raluan scoria fall deposit (after Nairn et al., 1989).*

At this locality there is a sharp contact between the scoria and the ignimbrite, while the upper surface of the ignimbrite is highly irregular. Deep channels have been infilled by Talili Pyroclastics, and overlying Rabaul Pyroclastics complete the sequence. The deposits of the Talili Pyroclastics record multiple (at least 7) smaller eruptions between the two most recent ignimbrite eruptions. At this locality there are at least 6 m of grey/pink weakly bedded and massive fine ashes with some pumice lapilli trains. These deposits are interpreted as pyroclastic surge deposits from water-modified intracaldera eruptions. Underlying beds include grey massive fine ash containing white dacitic pumice clasts, vesiculated fine ashes containing mudballs, and laminated dark and light grey ashes. Three soils and a strong unconformity are recognised in the Talili deposits at this locality. The scoria between the Talili deposits and the overlying Rabaul Pyroclastics is apparently from Palangiagia.

*Stop 13 — Raluan Pyroclastics, Talili Pyroclastics —Burma Road*

This is the type locality for both members of the Raluan Pyroclastics. Here about 2 m of pale yellowish-white rhyolitic ignimbrite overlies 0.5 m of black-brown basaltic scoria. Accretionary lapilli are present in the ignimbrite at this locality and at other more distal exposures. The scoria clasts scattered through the lower part of the ignimbrite may have been picked up during passage of the pyroclastic flow over the scoria deposit.

The overlying deposits are the mostly phreatomagmatic Talili Pyroclastics. The Talili deposits are at least 2 m thick here and are dominated by grey fine ashes. These deposits are commonly massive and friable but contain thin interbeds of hard fine ash, some of which show fine laminations. About 0.5 m above the base of the Talili deposits is a 0.3 m interval of hard, laminated and lenticular grey-yellow-brown fine ash beds with interbedded pumice trains. The presence of vesicles in the hard layers indicate they were wet when deposited. Two brown (weathered?) lithic-rich, pumice and ash layers about 0.2 m thick show signs of soil development.

The soil developed on the Raluan Ignimbrite and underlying the Talili Pyroclastics has given radiocarbon dates averaging at about 4400 yrs BP. A soil within the Talili Pyroclastics, near the top of the sequence, has

returned a $^{14}C$ age of about 1800 yrs BP. These dates indicate a significant period of repose (about 2400 years) following the Raluan Pyroclastics eruption. The sequence of Talili eruptions ended shortly before the Rabaul Pyroclastics eruption (1400 yrs BP).

*Stop 14 — Vunabugbug Pyroclastics, Talili Pyroclastics — Vunabugbug*

The Vunabugbug Pyroclastics comprise dacitic ignimbrite and Plinian pumice deposits. At this, the type locality, the Plinian pumice deposit overlies a strongly weathered soil. The Plinian deposit is about 0.3 m thick and consists of slightly reverse graded, weakly shower-bedded, loose pink/white pumice lapilli, coarse ash and black vitric clasts. The black vitric clasts give the deposit a characteristic speckled appearance. The Plinian deposit has been slightly to completely eroded along the outcrop by the overlying ignimbrite which is > 5 m thick at this locality. The ignimbrite is a light grey-white non-welded ash flow deposit containing scattered pumice lapilli. Radiocarbon dates from the soil beneath the Vunabugbug Pyroclastics indicate an age < 16,500 yrs BP.

Also exposed at this locality are the Talili Pyroclastics unconformably overlying the Vunabugbug deposits. All of the Talili deposits here are airfall and comprise multiple grey fine ashes, brown weathered scorias and pumice-bearing ash beds, with at least 5 included palaeosols. These deposits are overlain by the Rabaul Pyroclastics. The grey-brown vitric ash from the Talili sequence consists of fine (5-250 $\mu$m) glass shards and fragments which are weakly vesicular. Free crystals comprise plagioclase augite, hypersthene and Fe-Ti oxides. Bulk chemical composition is high-K dacite.

*Stop 15 — Kulau Ignimbrite, Kabakada Pyroclastics, Vunairoto Lapilli — Kabakada*

The Kabakada road cutting exposes a number of the "younger" pyroclastic deposits from Rabaul Volcano draped over a major unconformity on near flat-lying "older" deposits (Fig. 7). The unconformity is assumed to have an age of about 18,000 yrs BP (see background notes).

The Kulau Ignimbrite is the oldest of the "younger" ignimbrites exposed in this section. A basal Plinian pumice is absent both here and at a correlated section at Kerevat about 20 km to the south-southwest. The thickness of the Kulau Ignimbrite here exceeds 10 m while its Kerevat correlative is about 30 m thick. A characteristic feature of this deposit is the abundance of the lithic clasts that it carries. Pumice from the Kulau Ignimbrite is variable. Individual clasts are mostly mid to dark grey low-density, frothy pumice, but a small proportion are denser, charcoal grey, pumiceous cinder. Some of the larger clasts (up to 4 cm) are banded on a mm to cm scale with predominant mid-grey pumice streaked with thinner bands of denser grey-black material. Both light and dark pumices are crystal-poor. Phenocrysts are plagioclase, augite, hypersthene, Fe-Ti oxides and accessory apatite. The vesicular pale brown glassy base is crowded with microcrystals, particularly in the darker pumice. Very rare, anhedral quartz grains were found in one clast thin section. The bulk composition of pumice from the Kulau Ignimbrite is dacitic with relatively low $K_2O$ content.

The flat-lying pyroclastics at this locality include the Kabakada Pyroclastics Subgroup and the Vunairoto Lapilli. The Kabakada Subgroup incorporates all of the deposits between the Vunairoto Lapilli near the base of the section and the major unconformity beneath the Kulau Ignimbrite. It includes a basic Plinian scoria/acidic ignimbrite couplet near the base, overlain by grey and brown fine ashes interbedded with thin dacitic ignimbrites, and three Plinian pumice deposits at the top.

The Vunairoto Lapilli is a distinctive dark grey-brown Plinian pumice lapilli deposit. It overlies an intensely weathered palaeosol here. Consisting of weakly shower-bedded grey-brown lapilli and coarse ashes, with some interbedded fine ash bands, its thickness is about 1 m. The pumice lapilli analyses as high-K andesite.

*Stop 16 — Tavui Pyroclastics, Malaguna Pyroclastics — Tavui Fault Scarp*

The exposure at this locality is discontinuous occurring in a number of separate road cuts adjacent to and on the face of the Tavui Fault Scarp. The sequence includes unconformities and is broken and repeated by faulting.

Correlation between this and the previous locality has been made partly on the basis of field similarity of a pumice lapilli bed here and the Vunairoto Lapilli at Kabakada. The Kabakada Pyroclastics Subgroup is also tentatively correlated with some deposits here. In particular, an ignimbrite and underlying Plinian pumice in the upper part of the Tavui exposure contain yellow olivine of the same composition as the olivine in the uppermost Plinian deposit in the Kabakada Pyroclastics. In addition, there is a strong similarity between the mineralogy and chemistry of the pumice lapilli in both ignimbrite and Plinian deposits here and the Plinian deposit at Kabakada.

The presumed Vunairoto Lapilli deposit here is about 1 m thick. The general appearance of the deposit (clast lithology, grain size distribution, structure) is very similar to the Vunairoto Lapilli at Kabakada. However, the field evidence for correlation of the two deposits is

not well supported by chemical data. Pumice from the Tavui deposit is more siliceous (63.38%) and more K-rich (3.44%) than the material at Kabakada (60.68% $SiO_2$, 2.88% $K_2O$).

Underlying the presumed Vunairoto Lapilli is an undifferentiated set of deposits known as the Tavui Pyroclastics Subgroup. This Subgroup incorporates all of the pyroclastic deposits between the Vunairoto Lapilli and the Malaguna Pyroclastics. At this, the type locality, the Tavui Pyroclastics are about 5 m thick and consist of grey-green and grey fine ash deposits, overlain by a thin white ignimbrite and a Plinian pumice bed, with intervening palaeosols. These deposits underlie an intensely weathered palaeosol beneath the Vunairoto Lapilli. The Tavui Pyroclastics have not been positively identified elsewhere. They may be present under the Vunairoto Lapilli at Kabakada but with the Malaguna Pyroclastics absent there, the base of the Tavui deposits cannot be defined.

The Malaguna Pyroclastics outcrop near the base of this section. Pale-coloured silicic basal pumice beds are overlain by black welded ignimbrite of intermediate composition which grades upwards into grey non-welded ignimbrite. Details of these deposits are given in the notes for Stop 17.

The Tavui Fault scarp represents the only subaerial part of Tavui Caldera, the remainder of which lies offshore to the northeast. This arcuate scarp appears to cut Rabaul-erupted pyroclastic deposits, suggesting that both Rabaul and Tavui centres have been active over much the same period. However, no Tavui-sourced deposits have yet been positively identified, and all of the post-18,000 BP deposits in this area are from Rabaul.

## Day 4 Earlier Eruptives II

### *Stop 17 — Malaguna Pyroclastics — Tunnel Hill Road*

The Malaguna Pyroclastics constitute a widespread distinctive marker horizon around Rabaul. At this, (the type) locality, the formation is about 14 m thick but is displaced by several faults. From the base the restored section includes 3 m of pale grey-white Plinian pumice lapilli, grading up into as much as 8 m of weakly stratified dark grey-black sintered tuffs with some more-densely welded horizons. This passes into about 3 m of grey non-welded ignimbrite which contains some sintered bands and is pumice-rich in its lower 1 m. The basal contact of the Malaguna Pyroclastics is conformable on weathered grey fine vitric ashes and pumice beds, over older (?Boroi) ignimbrites. The upper contact is weathered and unconformable, and overlying deposits are poorly exposed.

The Malaguna Pyroclastics have a wider range of chemistry than any other Rabaul formation except for the Raluan Pyroclastics. Pumice from the basal Plinian unit analyses as high-K rhyodacite. Thin sections show phenocrysts of plagioclase, augite, hypersthene Fe-Ti oxides and accessory apatite in a colourless glass. The pumice clasts are nearly all uniformly pale coloured, but some pumices appear oxidised. Lithic content is low in the Plinian unit but includes accidental clasts of altered country rock and dark essential scoria clasts some of which have fused coatings of white pumice.

The dark moderately welded unit overlying the Plinian base comprises roughly banded, mm to cm size zones, which vary in welding intensity from thin layers of black glass to dark brown, open-textured scoriaceous pods. Angular, grey, lithic clasts are scattered throughout. Thin sections show phenocrysts of plagioclase, augite, hypersthene (Opx>Cpx) and Fe-Ti oxides in a very variable, but essentially vitric groundmass. Much of the rock comprises a jumbled mixture of juvenile material which includes clasts of hyalopilitic andesite, ash and lapilli of nearly colourless to nearly opaque glass with weakly vesicular to pumiceous texture, and shards and blebs of dark-brown glass. Compression, and distortion of vesicular material has occurred but only to a minor extent. Accessory, lithic andesitic clasts (up to 1 m in size) make up about 5% of rock volume. Chemical analysis shows the welded tuff to have a high-K andesite composition.

The non-welded grey ignimbrite forms a lapilli-rich layer immediately above the welded unit at this locality, and contains distinctive mixed, brown and grey pumice with straight tubular vesicles. The mixed material has shreds, strands and plates (up to 5 mm thick) of moderately vesicular, grey-white pumice incorporated in a micro-vesicular rather dense, brown glass. Within individual clasts, the grey-white pumice fragments are more or less aligned in the same direction within the dominant brown glass matrix, giving a striking banded appearance. The two components were not analysed separately, but the bulk composition of the banded, pumiceous, glassy lapilli is high-K andesite. The RI of the grey pumice glass is identical to that of the Malaguna plinian pumice, and therefore presumably has a similar, rhyodacitic chemistry.

The considerable chemical variation demonstrated in the Malaguna Pyroclastics at the type locality may explain the lack of precise chemical correlations to some field-correlated deposits elsewhere. Plagioclase from pumice of the Plinian unit has yielded an Ar-Ar date of 110 ka.

*Stop 18 — Latlat Pyroclastics, Talakua Pyroclastics —Talakua*

The Latlat Pyroclastics are dominated by a welded tuff which can be traced around the western and southern walls of Rabaul Caldera. At this locality in the south-southwestern wall of the caldera the basal pumice beds of the Latlat Pyroclastics contain cross-bedded surge deposits. Large black vesicular bombs to 0.4 m and spheroidally heat-spalled lithic andesite clasts to 0.2 m are found in these beds. The thickness of the basal pumice beds ranges up to 10 m where they infill fossil gullies in nearby sections. The overlying welded tuff and ignimbrite layers are about 15 m thick. Pumice from the ignimbrite at a correlated section about 4 km to the north is high-K dacite.

The greatest total thickness of the Latlat Pyroclastics occurs in sections a few km north of this location. The basal pumice bed clast size is also greatest in those sections as are surge cross-bedding parameters. These factors indicate that the caldera wall sections west-southwest of Vulcan Cone are closest to the source of the Latlat Pyroclastics.

Directly underlying the Latlat formation is the Talakua Pyroclastics Subgroup. At this locality these deposits attain a thickness of about 6 m. They consist of grey fine ashes and yellow brown Plinian pumice beds. Distinctive grey and white laminated fine ashes are also present. Slightly weathered, grey pumice from a Plinian deposit here is a high-K rhyodacite.

The Talakua Pyroclastics record a series of smaller-scale explosive eruptions occurring over an extended interval. At least 6 palaeosols occur between the fall deposits within the Subgroup.

At the base of the section is a compact pale pink-brown ignimbrite containing large (10 cm) pale grey-white pumice clasts having distinctive crystal clusters. Rounded, weathered lithic clasts are common in this deposit.

*Stop 19 — Varzin Depression —Tomavatur*

The present location is at the northern edge of the Varzin Depression, an 11 km wide subcircular feature south of Rabaul Caldera. The Varzin Depression is thought to represent the topographic expression of an early Quaternary caldera. Its northeastern boundary is linear and marked by the 6 km long northwest-trending eroded scarp of the Toma Fault. Arcuate lineations complete the outline of the depression, while other concentric arcuate lineations are present within the depression. A small eroded basaltic cone, Mt. Varzin lies near the eastern margin of the depression.

Farther south, beyond the Warangoi and Kerevat River valleys and in the Baining Mountains, are the late Tertiary volcanic centres responsible for the emplacement of the Nengmutka Volcanics. This formation is distributed over a 600 $km^2$ elongated area and consists of andesitic lavas and pyroclastic flow deposits, rhyolitic lavas, and derived sediments. The largest of the late Tertiary centres, the Nengmutka Caldera, hosts a series of north to northeast trending quartz veins that locally contain high grade gold-silver-telluride and copper-sulphide ore shoots.

*Stop 20 — Latlat Pyroclastics —Karavia Bay*

At this locality at the southern shore of Karavia Bay, the total thickness of the Latlat Pyroclastics is about 20 m. Pumice beds at the base of the formation are a few m thick. Pumice clasts include pale, pink-brown and dark brown-black varieties. Lithic clasts are abundant. The composition of pumice in the overlying ignimbrite is dacitic. Considerable compositional variation within the welded unit here is evident, from andesite to dacite. Welding at this locality is generally intense, with vitroclastic texture virtually obliterated in places.

Going west from this locality, the Latlat Pyroclastics rise progressively to about 300 m a.s.l. at the Talakua locality and then dip gently northwards along the western side of the caldera.

*Stop 21 — Karavia Welded Tuffs*

The Karavia Welded Tuffs are a sequence of grey tack-welded coarse fall deposits and black intensely welded crystal-vitric tuffs which are platy jointed. Less well-exposed correlated sections occur at somewhat higher elevations in the southwestern and southern walls of the caldera. The thickness at the present location is about 30 m although the upper and lower contacts are not exposed.

Abundant lithic clasts ranging up to about 1 m in size are subrounded to angular blocks of densely welded tuffs or lavas. These are enclosed in a scoriaceous glassy dacitic essential matrix.

The intensity of welding in this formation varies considerably. In places, sintered medium to coarse ash-sized crystal and lithic debris are roughly bedded on a mm to cm scale with black glass lenses. Densely welded platy tuff retains vitroclastic texture although shards are flattered, stretched and contorted, and in places, flow has occurred. The dark brown glass shows incipient spherulitic crystallisation locally.

The large clast sizes indicate proximity to source. However, this may be outside the present caldera,

perhaps in the Vunakanau area. Alternatively, the source may be inside the caldera in the Vulcan area.

The age of these deposits is unknown although they appear to be amongst the oldest pyroclastics at Rabaul.

*Stop 22 — Rabaul Quarry Lavas —Rabaul Town*

The Rabaul Quarry Lavas are mid-grey, strongly jointed rocks displaying arcuate to circular joint patterns at the present quarry workings. They pass eastwards into more massive platy jointed flows, some of which have scoriaceous bases. Lapilli sized inclusions are common.

The lava is porphyritic with abundant phenocrysts of plagioclase, augite, hypersthene, Fe-Ti oxides and apatite, commonly occurring as coarse clusters. The matrix has pilotaxitic texture, comprising plagioclase microlaths, specks of pyroxene, opaque oxides and hematite, and interstitial cryptofelsite. The laminations in the lava are discontinuous, sub-parallel pale grey to pale brown zones up to 1 mm thick and spaced a few mm to about 1 cm apart. These zones consist of either tridymite plus rare biotite or quartz plus olive-coloured amphibole and rare biotite. They probably represent crystallisation from vapour phase or deuteric fluids which filled cooling fractures.

The source of these lavas is unknown but was probably within the caldera. Lavas in the eastern wall of the caldera between Kombiu and Turangunan closely resemble these lavas in macroscopic and microscopic textures and in petrography and chemistry.

More massive lavas slightly east of the present location have been K-Ar dated - an age of 188 ka was obtained. Malaguna Pyroclastics overlie the Rabaul Quarry Lavas west of this location and Tovanumbatir Lavas appear to be older.